
Soft Robotic Eel

Major Qualifying Project

Advisors:

**CAGDAS ONAL
ROBIN HALL**

Written By:

**NATALIE ESSIG
CHRISTOPHER HUNT
PRANAV JAIN
DEXTER STARK**



WPI



**A Major Qualifying Project
WORCESTER POLYTECHNIC INSTITUTE**

This report represents the work of one or more WPI undergraduate students submitted to the faculty as evidence of completion of a degree requirement. WPI routinely publishes these reports on the web without editorial or peer review.

AUGUST 2024 - MAY 2025

ABSTRACT

Soft robotics offers a compelling approach to underwater locomotion, combining flexibility with bioinspired movement capabilities to navigate environments that challenge traditional rigid systems. This project aimed to create a cable-driven soft robotic eel based on, and seeking to improve upon, an earlier design developed by our advisor, Dr. Robin Hall. Building on this foundation, we focused on enhancing the eel's modularity, mechanical performance, and future expandability through iterative refinement of its segment architecture, actuation mechanism, and internal layout to support additional components. The robot consists of modular, 3D-printed accordion segments fabricated from thermoplastic elastomer filament, actuated using fishing line routed through each segment and wound around servo-driven spools to produce undulatory motion. This modular design facilitates straightforward customization, repair, and extension of the body. The system also includes a watertight head enclosure for electronics, soft passive fins, and a compliant tail to support natural swimming dynamics. The robot was tested in tank and pool environments to evaluate swimming speed and general operability in conductive, chlorinated water. While still requiring further development, this soft robotic eel establishes a modular and adaptable platform with strong potential for future research in bioinspired locomotion, environmental sensing, and underwater exploration.

ACKNOWLEDGEMENTS

We would like to extend our gratitude to our advisor, Professor Cagdas Onal, for his guidance, feedback, and resources throughout this project. We also sincerely thank our co-advisor, Dr. Robin Hall, for his mentorship, technical insight, continued support, and generosity in lending equipment and supplies from his own work. Additionally, we appreciate the assistance provided by everyone in the WPI Soft Robotics Lab (SRL), whose help was crucial in accessing resources and troubleshooting. Lastly, we thank Worcester Polytechnic Institute for the financial support that made this project possible.

TABLE OF CONTENTS

ABSTRACT.....	1
ACKNOWLEDGEMENTS.....	2
TABLE OF CONTENTS.....	3
LIST OF TABLES.....	5
LIST OF FIGURES.....	6
1 INTRODUCTION.....	8
1.1 Objectives:.....	8
2 BACKGROUND.....	10
2.1 Advantages of Soft Aquatic Robots.....	10
2.2 Anguilliform Motion.....	10
2.3 Prior Work and Context: Underwater Robotics and Hall's Soft Eel Systems.....	13
2.4 Fins in Eels and Robotic Design.....	14
2.5 Eel Biology and Research Relevance.....	15
2.6 Robotic Fish.....	15
3 METHODOLOGY.....	16
3.1 Mechanical Design.....	16
3.1.1 Mechanical Design Philosophy.....	16
3.1.2 Head.....	17
3.1.2.1 Head Waterproof Testing.....	18
3.1.3 Body Modules.....	18
3.1.3.1 Accordion.....	20
3.1.3.2 Hex Caps.....	23
3.1.3.3 Spacers.....	25
3.1.3.4 Motors.....	26
3.2 Controls.....	27
4 IMPLEMENTATION.....	29
4.1 Overview.....	29
4.1.1 Bill of Materials.....	29
Head Segment.....	29
Modular Body Segments.....	30
Tail Segment.....	30
4.2 Mechanical Structure.....	30

4.2.1 Head.....	30
4.2.2 Modules.....	32
4.2.3 Tail.....	34
4.2.4 Fins.....	35
4.3 Electronic Design.....	36
4.3.1 Control Board.....	36
4.3.2 Wiring.....	36
4.3.3 Servo Motors.....	38
4.3.4 Battery.....	39
4.4 Applications.....	40
5 TESTING AND RESULTS.....	41
5.1 Accordion Material Testing.....	41
5.2 Spool String Wraps.....	43
5.3 Servo Amplitude/Speed Testing.....	44
6 DISCUSSION.....	47
6.1 Comparison to Previous Eel.....	47
6.2 Challenges.....	47
7 RECOMMENDATIONS.....	48
7.1 Overview.....	48
7.2 Mechanical Design.....	48
7.3 Electronic Hardware.....	49
7.4 Controls.....	49
7.5 Future Exploration.....	50
8 CONCLUSION.....	51
8.1 Importance.....	51
REFERENCES.....	52

LIST OF TABLES

Table 3.1: Accordion design iteration parameters and bend angle proxy (Hypothetical Bend Angle)	23
Table 3.2: A table of the various iterations of the hex cap throughout the design process	25
Table 5.1: Table of results from testing body module bend angles with accordions made from Chinchilla and NinjaFlex	43
Table 5.2: Table of results from testing body module bend angles with different amounts of spool wrapping	44
Table 5.3: Table of data collected from Servo Amplitude vs Speed Testing	46

LIST OF FIGURES

Figure 2.1: A modeled anguilliform waveform showing increasing lateral displacement from head to tail, based on a traveling sine wave with nonlinear amplitude growth	12
Figure 2.2: DRAGON, a soft-bodied robot developed by Hall et al. (2024), featuring multi-cable actuation and a modular accordion segment.....	14
Figure 2.3: Hall's 2023 tetherless soft robotic eel, with a water-tight electronics head, spring-based backbone, and cable-driven servo actuation.....	14
Figure 3.1: The final iteration of the fully assembled EEL	16
Figure 3.2: The head shown within the context of the final robot.....	17
Figure 3.3: Waterproof testing of the watertight compartment in the head	18
Figure 3.4: The middle body module shown within the context of the final robot	19
Figure 3.5: Zoomed-in view of the body module	19
Figure 3.6: The accordion of the middle body module shown within the context of the middle body module.....	20
Figure 3.7: Screenshot of the SolidWorks model of the accordion with an overlay of the bend angle approximation sketch (top), and the parameter table (bottom)	22
Figure 3.8: The motor side hex cap of the middle body module shown within the context of the middle body module	23
Figure 3.9: The middle body module spacer shown within the context of the middle body module.....	26
Figure 3.10: A spacer with the motor mount attached, with floats and weights attached	26
Figure 3.11: Left: silicone grease applied to the circuit board of the motor. Right: 3M Marine Fast Cure Adhesive Sealant on the outer edges of the motor	27
Figure 4.1: The cover, board compartment, and battery compartment of the head	31
Figure 4.2: The fully assembled head, including housing for the depth control	31
Figure 4.3: Complete body module	33
Figure 4.4: CAD model of the spool.....	34
Figure 4.5: Passive Tail Assembly and Mount with Drainage and Buoyancy Holes	35
Figure 4.6: CAD model of one of the fins	35
Figure 4.7: Perf board, ESP32, and L293D	36
Figure 4.8: Wire connections found in each module	37
Figure 4.9: Full wiring layout including waterproof connectors and assembled segments.....	37

Figure 4.10: Wiring diagram used for signal and power distribution throughout the robot	38
Figure 4.11: Steps to seal each motor, and the placement of each sealant.....	39
Figure 4.12: The fully waterproofed battery	40

Figure 5.1: Body modules made of Chinchilla and Ninjaflex set up for bend angle testing	42
Figure 5.2: Diagram of the geometry utilized to calculate bend angle	42
Figure 5.3: Pool testing of the soft robotic eel during servo amplitude trials.....	45
Figure 5.4: Screenshot of Physlet Tracker being used to determine Eel speed	45
Figure 5.5: Graph of eel speed in body lengths per second vs the servo amplitude in degrees...	46

1 INTRODUCTION

Aquatic robotic systems are increasingly valuable tools for underwater exploration, research, and environmental monitoring. However, traditional robots often struggle in complex environments as they are rigid, bulky, and disruptive to delicate ecosystems [1]. To address these limitations, we focused on developing a soft, bioinspired robot that emulates the efficient, flexible locomotion of eels [2].

Soft robotics offers unique advantages for underwater systems. These robots are inherently compliant, enabling safe interactions with fragile surroundings, and they excel in tight or cluttered environments where traditional rigid-bodied robots may fail [3]. Their ability to mimic the smooth, continuous motions of biological swimmers makes them especially suited for ecological monitoring, inspections in confined spaces, and studies of biomechanics in the field [4].

This project builds upon previous work by our co-advisor, Dr. Robin Hall, who developed a tetherless, cable-driven soft robotic eel. Our goal was to improve upon this design in three main areas: mechanical modularity, swimming performance, and future expandability. We wanted to create a platform that was not only functional, but also easy to iterate on to enable future research.

Our final prototype consists of modular, 3D-printed segments actuated via fishing line wrapped around servo-powered spools. The robot undulates like a real eel, with each segment contributing to the wave-like motion. Key features include a flexible body printed in NinjaTek Chinchilla TPE, waterproofed servos, and a watertight electronics head housing. The result is a biologically inspired platform with the potential for remote or autonomous underwater tasks.

1.1 Objectives:

This project aimed to develop an improved version of the tetherless soft robotic eel developed by Dr. Hall, focusing on the following key objectives:

1. **Enhance Modularity:** Design body segments as independent, interchangeable modules to simplify repair, customization, and future upgrades.
2. **Increase Mechanical Performance:** Achieve comparable or superior performance to the original design in measurable metrics such as swim speed, bend amplitude, and durability.
3. **Enable Future Expandability:** Create a platform capable of supporting additional sensing, control, and navigation systems. These may include acoustic communication modules, depth and orientation sensors, environmental monitors, and buoyancy control mechanisms.

2 BACKGROUND

2.1 Advantages of Soft Aquatic Robots

Bio-inspired soft aquatic robots provide multiple significant benefits over their rigid counterparts, including enhanced durability, minimal environmental disruption, improved navigability in complex spaces, and more accurate replication of biological motions [5]. Regarding resiliency, soft robots have two main advantages over rigid robots: first, soft robots can more readily adapt to high-pressure environments like those seen in deep-sea exploration [6]. Second, their compliance allows them to absorb and dissipate impacts, allowing them to mitigate the effects of impacts better than rigid robots of similar quality [7].

Soft robots, especially those with non-thruster-based propulsion mechanisms, have reduced mechanical and acoustic signatures [2]. This allows them to observe organisms that may otherwise be startled or maintain the integrity of fragile environments such as shipwrecks or coral reefs. In addition, soft robots are often smaller and more maneuverable in tight spaces [2], making them ideal for navigating complex areas. Finally, soft robotics allows for more accurate replication of biological motions, making them valuable platforms for studying biomechanics [4].

2.2 Anguilliform Motion

The motion that allows eels to generate propulsion through water is known as anguilliform motion, or anguilliform swimming. Propulsion is achieved through a smooth undulatory wave that travels down the length of the body, generating vortices that jet water backward and, through Newton's third law, propel the eel forward [8]. This gait provides efficient propulsion and high maneuverability, especially at low speeds [9,10]. Full-body flexibility also allows for tight turns and navigation through cluttered environments [11], complementing the strengths of soft robots. Moreover, anguilliform motion enables bidirectional locomotion simply by reversing the traveling wave [8]. This mechanical simplicity is particularly

Background

well suited to soft robotics, where actuators can bend back and forth without requiring complex limb-like systems [12].

Anguilliform motion is one of several body-caudal fin (BCF) gaits observed in fish, each offering different tradeoffs between speed, efficiency, and agility [13]. Thunniform swimmers like tuna and sharks concentrate most of their motion in the caudal fin, allowing for highly efficient, sustained high-speed travel. Carangiform swimmers, such as mackerel and jackfish, rely on undulations in the posterior third of the body for a balance of efficiency and thrust. Subcarangiform swimmers, such as trout and salmon, maintain a relatively rigid anterior body with increasing undulation amplitude toward the tail, optimized for upstream swimming. In contrast, anguilliform swimmers like eels, lampreys, and catfish generate wave-like motions along nearly their entire body length, allowing for unmatched maneuverability in narrow or complex environments [8].

This motion can be modeled as a sinusoidal traveling wave of the form:

$$y(x, t) = A(x)\sin(kx - \omega t)$$

where $y(x, t)$ is the lateral displacement at position x and time t , $A(x)$ is the amplitude function, k is the wavenumber, and ω is the angular frequency. The amplitude function typically increases from head to tail, modeled as:

$$A(x) = A_0 + (A_{max} - A_0)\left(\frac{x}{L}\right)^n$$

where A_0 is the minimum amplitude, A_{max} is the tail amplitude, L is the total body length, and n controls growth rate [10]. This waveform, with amplitude increasing along the body length, reflects the way eels generate propulsion through traveling body waves. A visual representation of this modulated sine wave is shown in Figure 2.1.

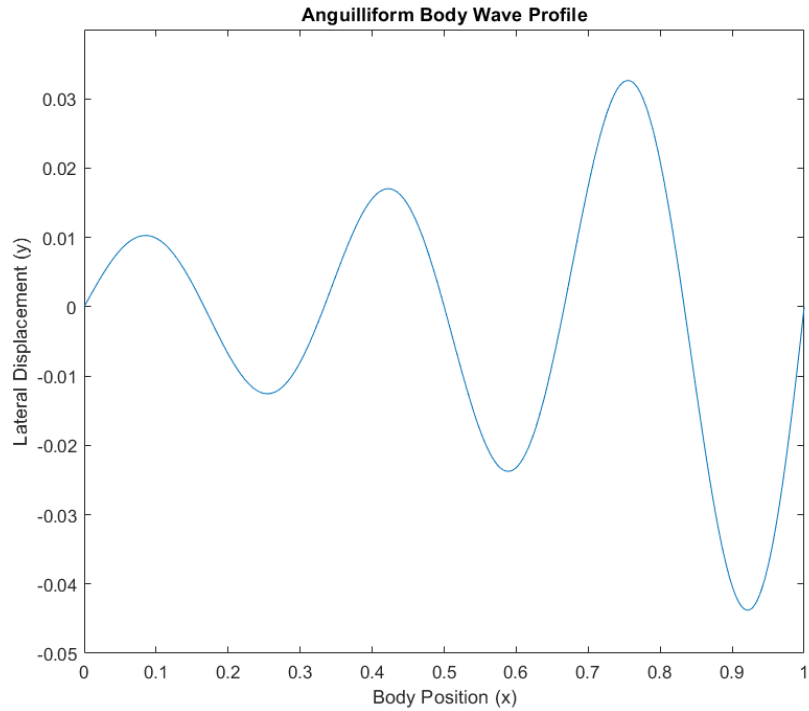


Figure 2.1: A modeled anguilliform waveform showing increasing lateral displacement from head to tail, based on a traveling sine wave with nonlinear amplitude growth.

This biologically inspired gait translates exceptionally well to soft robotic systems. Because anguilliform locomotion relies on smooth, continuous body waves rather than discrete joints or fin mechanisms, it maps naturally onto modular, flexible designs. This modeling approach has been used in multiple robotic platforms, where time-based sine waves drive body segments to emulate eel-like motion [14,5]. In our robot, each 3D-printed segment is actuated to follow a time-based sine wave, producing realistic eel-like motion through simple, repeated control patterns. This enables the robot to move fluidly through confined spaces, avoid bulky or noisy hardware like propellers, and minimize disturbance to its surroundings, which are key advantages for delicate aquatic environments, ecological monitoring, and bioinspired exploration [2].

2.3 Prior Work and Context: Underwater Robotics and Hall's Soft Eel Systems

Underwater robots are typically categorized as Remotely Operated Vehicles (ROVs), Autonomous Underwater Vehicles (AUVs), and biomimetic systems. ROVs are tethered and controlled from the surface, AUVs operate independently using onboard autonomy, and biomimetic systems aim to replicate the efficient, adaptable movements of aquatic organisms [15,13].

Two soft robotic eel platforms developed by Dr. Robin Hall are *DRAGON* (Design for Robust Autonomous Gaited Operation in Nature) and the *Tetherless Soft Robotic Eel* [16]. While developed as separate projects, both explored modular cable-driven architectures for soft-bodied anguilliform locomotion. DRAGON prioritized robust integration of onboard power and control systems for untethered operation, whereas the tetherless eel emphasized simplified fabrication, segment-level modularity, and rapid prototyping for academic testing.

Our MQP is a direct continuation of the tetherless eel platform, but it also drew critical inspiration from DRAGON. Although DRAGON is not an eel, its mechanical design, particularly the use of soft accordion-style segments and multi-cable actuation, informed our approach to modularity and actuation (see Figure 2.2). These features were adapted to improve modularity, manufacturability, and stability in our own implementation.

The tetherless eel, shown in Figure 2.3, featured a watertight electronics head, wave-spring body design, and 180-degree servo motors coupled to spools that actuated internal cables. It achieved a top speed of 0.2 body lengths per second and bend angles ranging from 26.4° to 56.7° , depending on segment and direction according to R. Hall [16], (personal communication, Aug. 2024–May 2025). While effective, it lacked remote control, sensor integration, and vertical mobility, and it faced limitations in motor reliability and electronics access. Our system builds upon this foundation with improvements in modularity, actuation architecture, and expandability for future research.



Figure 2.2: DRAGON, a soft-bodied robot developed by Hall et al. (2024), featuring multi-cable actuation and a modular accordion segment [16]

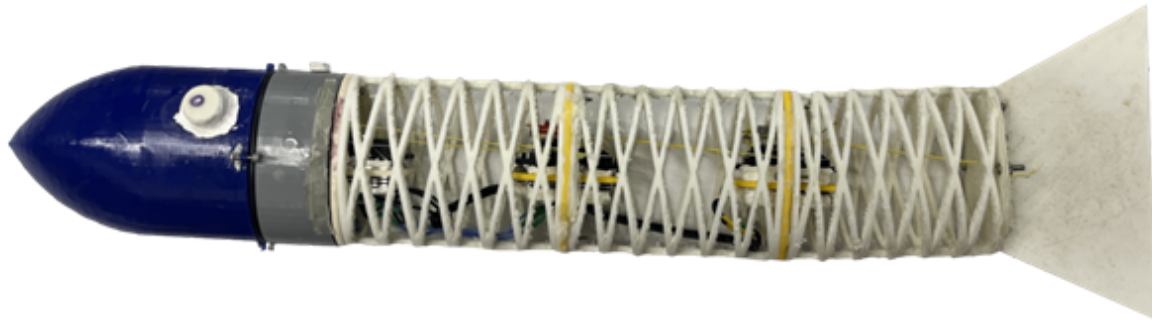


Figure 2.3: Hall's 2023 tetherless soft robotic eel, with a water-tight electronics head, spring-based backbone, and cable-driven servo actuation [16]

2.4 Fins in Eels and Robotic Design

In biological eels, fin structures contribute to stabilization and maneuverability rather than propulsion. Most species possess continuous dorsal, caudal, and anal fins that are fused into a single undulating ribbon along the body's upper and lower surfaces. These fins help reduce rolling, support hovering, and improve turning control, particularly during slow swimming or reverse motion [17,18]. Unlike pectoral fins in many other fish, eel fins are flexible, elongated, and closely integrated with the body's midline. Their passive interaction with fluid flow allows them to function as dynamic stabilizers in cluttered or confined environments. Prior studies in

both biology and robotics suggest that the presence of such fin structures, whether actuated or passive, can enhance directional stability and reduce energy loss caused by lateral drift [19]. For soft robotic systems aiming to replicate anguilliform motion, incorporating fin-like elements may offer a low-complexity strategy to improve swimming consistency in naturalistic conditions.

2.5 Eel Biology and Research Relevance

Eels are elongated, muscular fish known for their ability to navigate confined or complex environments such as coral reefs, rocky crevices, and dense aquatic vegetation [20]. Their locomotion strategies, particularly anguilliform swimming, enable efficient, precise movement in cluttered habitats. Some species, like the American eel (*Anguilla rostrata*), undertake long-distance migrations from freshwater rivers to marine spawning grounds, but these journeys remain poorly understood, largely due to challenges in tracking eels in the wild [21]. Despite their ecological and biological significance, eels remain under-studied relative to other aquatic species due to challenges in tracking their full life cycle, particularly their oceanic spawning phase [22]. This gap in understanding is partly due to the limitations of current observation tools [23]. A soft robotic eel capable of emulating real eel motion offers a promising platform for studying eel biomechanics, behavioral patterns, and environmental interactions in a noninvasive, biologically relevant manner.

2.6 Robotic Fish

Robotic fish are a class of underwater robots that emulate the swimming mechanics of real fish in order to improve agility, efficiency, and environmental compatibility [24]. These systems often use flexible bodies, articulated linkages, or soft actuators to replicate biologically accurate gaits such as thunniform, carangiform, or anguilliform motion [13]. Compared to thruster-based systems, robotic fish produce significantly less mechanical and acoustic noise, making them better suited for applications in ecological monitoring, stealth inspection, or marine life interaction [2,4]. Soft robotic fish in particular benefit from compliance and adaptability, enabling safe interaction in delicate or sensitive environments [5]. Our soft robotic eel fits within this growing domain of biologically inspired underwater systems, offering a modular, tetherless solution that mimics natural undulatory swimming.

3 METHODOLOGY

Our team began by doing extensive research to understand the design of various types of underwater soft robots, especially robotic eels. We also talked with our co-advisor, who had worked on the first version of this project, to see what had already been done and how we could make improvements. Based on our research and these conversations, we came up with a few initial goals. While the specifics of these goals changed throughout the project, the core concept of creating a tetherless soft robotic eel, with an emphasis on modularity and improved performance, stayed consistent. To achieve this, we divided the Eel into various components that would need to be designed and manufactured. Our team utilized 3D printing to rapidly prototype and iterate on these components.

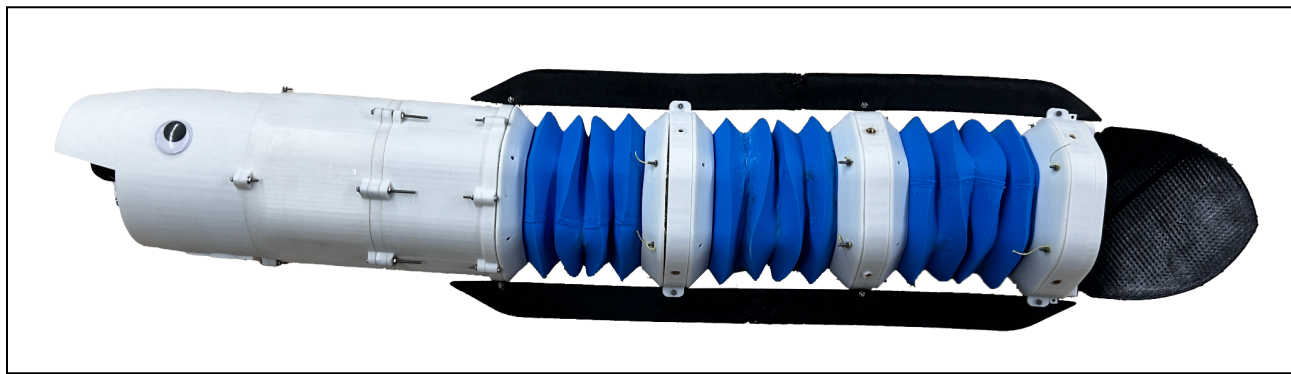


Figure 3.1: The final iteration of the fully assembled EEL

3.1 Mechanical Design

3.1.1 Mechanical Design Philosophy

Our mechanical design philosophy was shaped by our goals, budget constraints, and lessons learned from the previous iteration. Our MQP budget was 1,000 USD, which meant all the testing and building of the final product needed to be done within this cost limitation. To

improve on the previous project, we wanted the robot to have a greater angle of undulation and make it swim faster in the water. To make the eel easier to recreate and modify in the future, we focused on the modularity of the eel's sections and used WPI's Soft Robotics Lab and the Prototyping Lab to 3D print all the parts. We also decided not to make the eel completely waterproof, as it would be really difficult to make, and a small hole in the eel could result in irreversible damage. Instead, we decided to only waterproof the vital parts within the eel, such as the wires, battery, and servo motors, and house the control board in a water-tight compartment.

3.1.2 Head

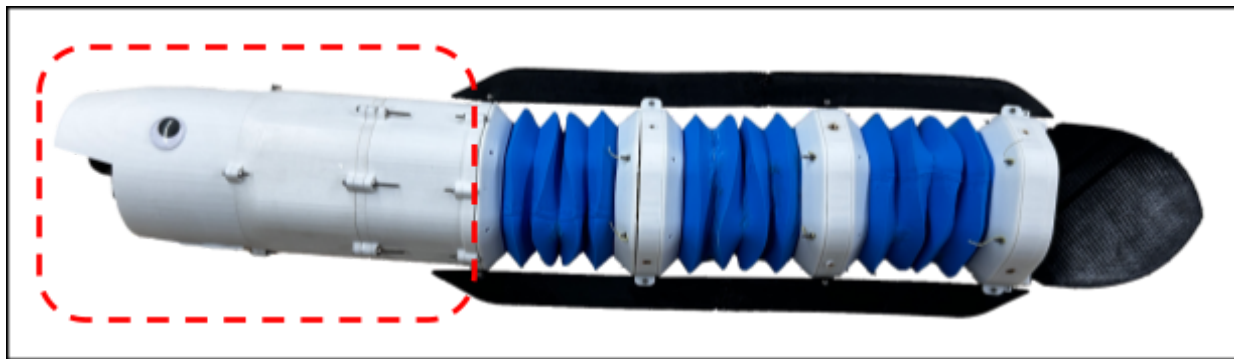


Figure 3.2: The head (circled in red) shown within the context of the final robot

The head was designed to house all non-motor components essential to the eel's operation, including electronics boards, batteries, switches, and potential future modules for sensing and buoyancy control. The head underwent extensive iteration to ensure functionality, accessibility, and watertight integrity. The initial design was a single elongated unit with internal dividers to isolate sensitive components. Its outer geometry transitions from an oval to a horizontally compressed hexagon as the head goes from the front towards the body, improving hydrodynamic efficiency and simplifying integration with the hexagonal body modules.

To improve internal access and ease of assembly, the final design was divided into three parts: the front houses the battery and main power switches; the middle contains a watertight compartment for the electronics; and the rear connects structurally to the body. Although time constraints prevented the full implementation of onboard sensors and a buoyancy control system, mounting points and internal space were included in the design to support these upgrades in future iterations.

3.1.2.1 Head Waterproof Testing

The section of the eel that needed to be waterproofed was the mid-section of the head with all the circuitry. Hence, the compartment and its lid were 3D printed using PLA, covered in acrylic coating, and an O-ring was added to the cover of the compartment. The lid was then screwed in. There were some holes in the compartment to allow the wires to be connected to the motors, battery, etc. Hence, hot glue was put on these holes to test the water-tight compartment. This section of the head was then put underwater and shaken to see whether any air bubbles emerged. Next, the outside of the compartment is dried with a towel and the screws are removed. We tested the seal integrity using dry tissue paper inside the compartment and checked for any signs of moisture post-submersion.

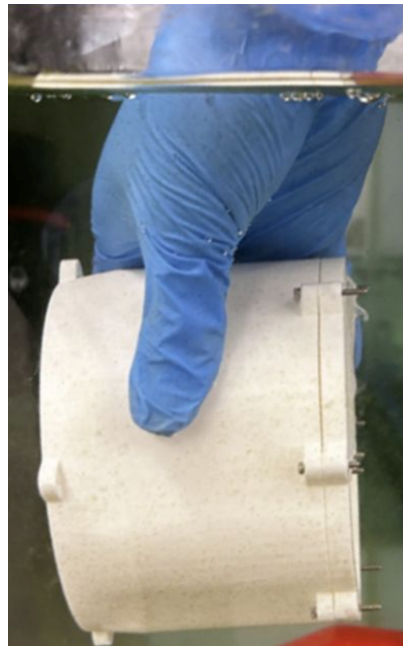


Figure 3.3: Waterproof testing of the watertight compartment in the head

3.1.3 Body Modules

Another core component of the eel is its body modules, which, like the head, underwent extensive redesign and iteration throughout the project. Each module was designed to produce anguilliform motion using a cable-driven mechanism, in which a servo motor rotates a spool to pull on one side of a pair of strings while releasing the other. This uneven pulling motion causes the flexible accordion structure to bend between two rigid hex caps. The design evolved significantly across multiple prototypes to optimize bend angle, reduce string tension, improve

Methodology

structural reliability, and streamline integration with the rest of the system. The Key elements of these modules are the accordion section, hex caps, motor spool, and support spacers, each of which was individually refined to balance performance, printability, and ease of assembly.

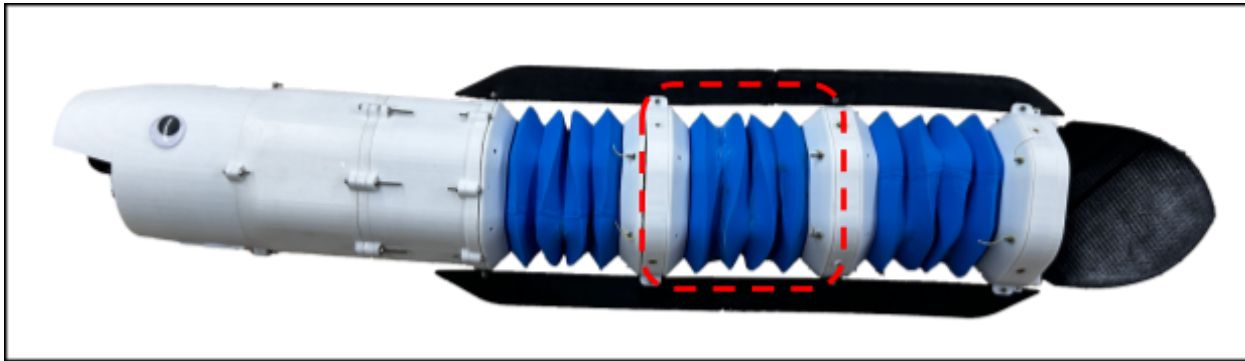


Figure 3.4: The middle body module (circled in red) shown within the context of the final robot



Figure 3.5: Zoomed-in view of the body module

3.1.3.1 Accordion

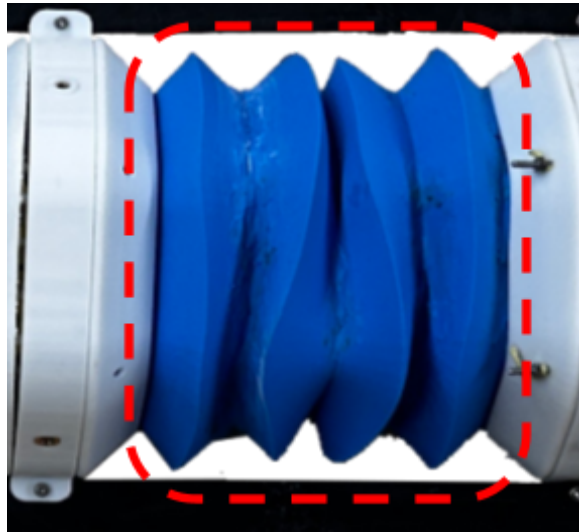


Figure 3.6: The accordion of the middle body module (circled in red) shown within the context of the middle body module

The accordion is the soft section of the eel, fabricated from NinjaTek Chinchilla filament, and is responsible for generating the sinusoidal motion that propels the robot forward. Because prior work by our advisor, Dr. Hall indicated that increased bend angle correlates with faster swimming speed [16], we prioritized maximizing the bend angle in our accordion design. To explore how specific design parameters influenced bending performance, we developed a heavily parameterized SolidWorks model. A separate sketch was used to approximate the bending geometry, enabling rapid iteration and providing a proxy value closely related to the actual bend angle (see Figure 3.7).

This approximation relied on two simplifying assumptions: (1) the uncompressed side of the accordion remains at a fixed length, and (2) the folds on the compressed side collapse completely onto each other without compressing beyond the material's thickness. Based on these assumptions, the compressed height of the accordion was estimated using the number of ridges and the thickness of each fold. With the calculated compressed height and known geometry of the shorter side, the sketch estimated the overall bend angle of the accordion.

This model highlighted several ways to increase the estimated bend angle: increasing the ratio between the uncompressed and compressed sides, extending the uncompressed height, reducing the compressed height, decreasing the number of ridges, and narrowing the base width.

From all these possibilities to increase the bend angle, it was impractical to decrease the base side width, as doing so would reduce the tube volume and cross-sectional area, limiting our

Methodology

designs for the rest of the eel. The first method we explored to improve the bend angle was to decrease the number of ridges. This could be practically achieved in two main ways: increasing the ridge width, which subsequently increases the vertical distance covered by each ridge, decreasing the ridges per unit of height, or increasing the ridge angle. Decreasing the ridge width had diminishing returns and eventually ended up decreasing the bend angle at 20mm. (see Iteration 1 in Table 3.1) The ridge width also decreased the usable volume/cross-section of the tube; thus, 15mm was selected as a nice value that still had significant improvement over 10mm. (see Iteration 2 in Table 3.1). The original ridge angle we started with was around 30° . This resulted in a significant droop of the part when printing because 3D printers are designed to print at 45° angles and higher for overhangs. However, increasing the angle too much negatively impacted the bendability of the accordion, so an angle of 45° was selected. (see Iteration 3 in Table 3.1)

Our team also decided to increase the total height by 25% from the original design because it resulted in a significant increase in the bend angle from 53.97° to 70.2° (see Iteration 4 in Table 3.1). Increasing the total height further would have continued to improve the bend angle; however, our initial prints with soft materials displayed increasing potential for failure with longer print times. Hence, we decided not to increase it beyond that point.

Methodology

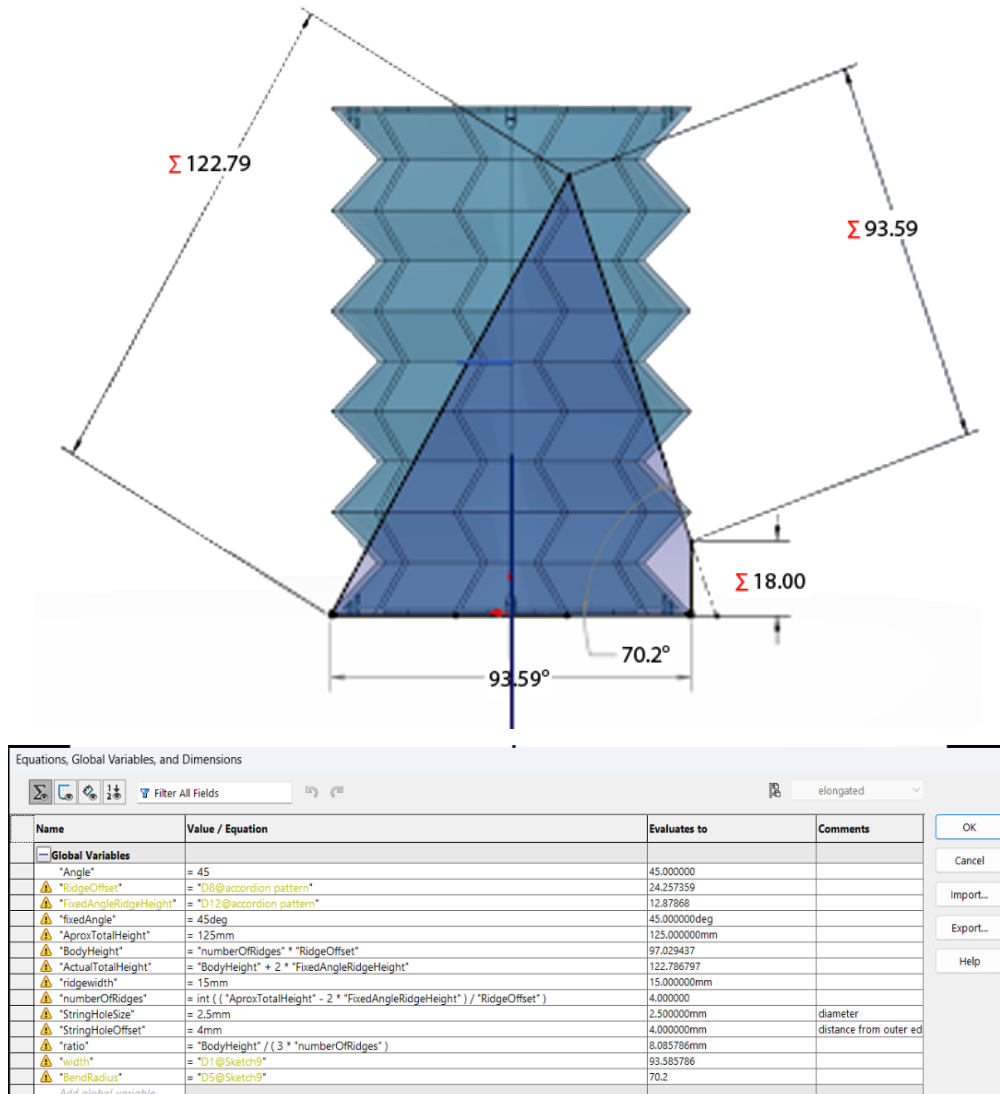


Figure 3.7: Screenshot of the SolidWorks model of the accordion with an overlay of the bend angle approximation sketch (top), and the parameter table (bottom)

Methodology

Iteration	0	1	2	3	4
Hypothetical Bend Angle (deg)	38.13	45.27	47.19	53.97	70.20
Height (mm)	100	100	100	100	125
Ridge width (mm)	10	20	15	15	15
Ridge angle (degrees)	30	30	30	45	45

Table 3.1: Accordion design iteration parameters and bend angle proxy (Hypothetical Bend Angle)

3.1.3.2 Hex Caps

The hex caps are rigid sections made from PLA and attached to either side of the accordion. These caps had several design iterations to improve performance, reduce string tension, and optimize structural efficiency.

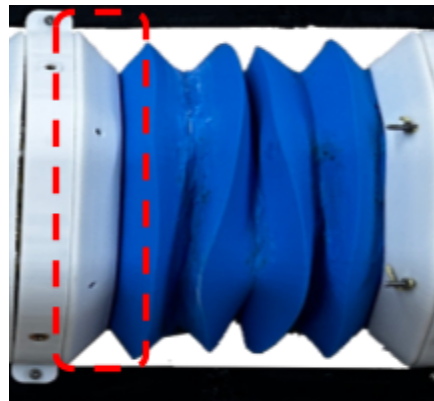


Figure 3.8: The motor side hex cap of the middle body module (circled in red) shown within the context of the middle body module

Methodology

The initial hex cap design involved routing the control strings from the passive side, through holes in the accordion, and into the motor side. A notch was included on the motor side to allow the two strings to converge before entering the pulley system, reducing the need for two separate pulleys as seen in Iteration 1 of Table 3.2. While this reduced mechanical complexity, the 90° bends introduced by the notch increased string tension significantly. Furthermore, the design required excessive filament to support the motor mount and was structurally weak, making it prone to breakage under load.

To address these issues, the motor side was redesigned with 3 notches at 30° intervals, allowing for a more gradual bending of the string path and reducing tension. The motor mount was also separated into its own component to reduce filament waste and print time, as seen in Iteration 2 of Table 3.2. Additional holes were introduced to test the optimal motor positioning. This iteration saw improved strength and reduced string tension, but even with a high-torque motor, the tension still limited the accordion's bend angle.

In the next version, Iteration 3, redundant holes on the motor side were removed, making the cap thinner and freeing up internal space for other components. Although this improved compactness, string tension remained a limiting factor. To further reduce this tension, the convergence point for the strings was moved from the motor side to the passive side (see Iteration 4 of Table 3.2). This change eliminated the need to use the notches on the motor side and allowed the motor to rotate ~120° in either direction, greatly improving the range of motion. However, this increased rotation speed caused the strings to pop off the pulley system, reducing the reliability of the eel's movement.

To counteract this, in Iteration 5, slots were added to the motor side to contain the strings and prevent them from derailing during rapid movement. While this improved the robot's performance, the string retention components were difficult to secure due to limited space and were susceptible to breakage because of their height. In the final iteration, these slots were reengineered as snap-fit features reinforced with screws for added strength. A slot was also introduced on either side to house the I2C to PWM circuit, as seen in iteration 6 of Table 3.2; however, due to the time limitations of the project, our team decided to drop this idea. This slightly impacted the ease of modularity of the eel but simplified the project.

Methodology

Iterations	1	2	3	4	5	6	7
Motor Side							
Passive Side							

Table 3.2: A table of the various iterations of the hex cap throughout the design process.

3.1.3.3 Spacers

The spacers are also made of PLA and were initially used to provide clearance for the string tensioning modifications on the hex caps. Their design evolved alongside multiple hex cap iterations and later expanded to include additional functionality. Examples include attaching foam or weights to achieve neutral buoyancy, supporting the motor mounts, and serving as mounting points for the fins. One spacer also acts as an adapter between the head and the first body module, while any spacer, including earlier versions without motor supports, can be used to connect the last module to the tail, where no motor is present.

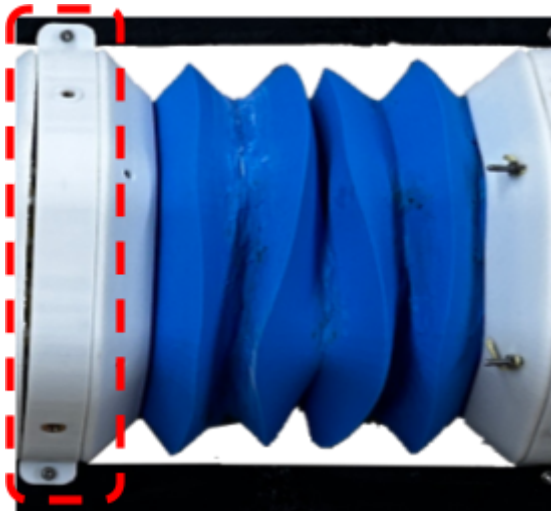


Figure 3.9: The middle body module spacer (circled in red) shown within the context of the middle body module



Figure 3.10: A spacer with the motor mount attached(yellow), with floats and weights attached

3.1.3.4 Motors

Our team aimed to improve the bend amplitude (i.e., the maximum bend angle) of the previous eel. The previous project used A62BHL, a high-torque servo motor capable of 180° of motion. To improve the bend angle, we decided to use servos with a wider range of motion, such

as 360° or continuous rotation servos. Our team landed on Parallax Feedback 360° High-Speed Servos, which were cheaper and had 360° of continuous rotational motion and absolute encoders. However, these motors were not designed for underwater use and required waterproofing for our application. Initially, our team utilized the waterproofing technique used by our co-advisor on the previous iteration of this project. These procedures involved using 3M 5200 marine sealant to cover all the holes where water might seep into, such as screw holes and seams. We also put an o-ring on the shaft under the servo horn. However, water still managed to enter the servos, short-circuiting the boards. To improve the waterproofing process, we opened the servos so we could waterproof them from the inside out. For this, we used 3 different types of grease: NyoGel, Super Lube, and silicone grease. NyoGel is quite hydrophobic but should be used for relatively slower-moving parts. Super Lube is less hydrophobic and can be used for faster-moving parts, and silicone grease should generally be avoided on moving parts. The step-by-step waterproofing can be seen in the implementation section.

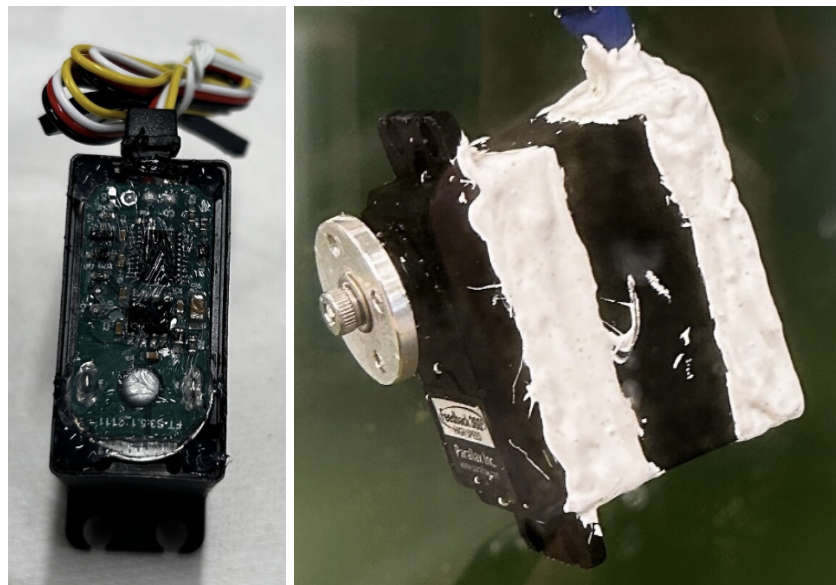


Figure 3.11: Left: silicone grease applied to the circuit board of the motor. Right: 3M Marine Fast Cure Adhesive Sealant on the outer edges of the motor.

3.2 Controls

Our team gave a higher priority to the mechanical aspect of the project. Hence, to control our robot, we hard-coded our robot to use the sine-wave function to determine the angle that each servo should be at. The sine-wave function is

Methodology

$$\text{Angle} = A \sin(\omega t - \varphi)$$

where A is the amplitude, ω is the angular frequency, t is time, and φ is the phase shift. The servo was then sent to that angle, which allows each module to keep bending. The formula for the discrete phase shift is

$$\text{Phase Shift} = \frac{2\pi}{\text{Number of Modules}}$$

As our team ended up using 3 modules, our phase shift was $\frac{2}{3}\pi$. This allowed for a nice-looking sinusoidal movement from the eel to be generated when all the modules were joined together. Our team chose a frequency of 1.25 Hz as it was the same frequency as biological eels and worked well for the previous project.

4 IMPLEMENTATION

4.1 Overview

In its final iteration, the robot consists of five main sections: a battery compartment, control board compartment, future depth control housing, three active propulsion modules, and a passive tail. The full assembly measures approximately 814 mm in length. Several key components, such as the ESP32, voltage regulator, syringe, perf board, and screws, were provided at no cost by the Soft Robotics Lab. The remaining parts used in the final build cost approximately \$240.

4.1.1 Bill of Materials

All remaining structural components of the eel, aside from the items listed below, were custom-designed and 3D printed using either PLA (for rigid parts) or TPE (for flexible elements).

Head Segment

- 1 × ESP32 microcontroller
- 1 × L293D motor driver
- 1 × Voltage regulator (compatible with 7.4 V input)
- 1 × 7.4 V rechargeable battery
- 1 × DC motor with integrated lead screw
- 1 × Transistor switch
- 1 × Syringe (used for linear actuation)
- 1 × O-ring
- 1 × Threadlocker
- 1 × Waterproof wire connector set
- 8 × M2 heat-set inserts

Modular Body Segments

- 1 × 360° servo motor
- 1 × Metal servo horn
- 1 × High-tensile string (for tendon actuation)
- 4 × M4 heat-set inserts
- 6 × M4 screws with matching nuts
- 5 × M3 screws
- 10 × M2 screws with matching nuts
- Electrical wiring
- Super Lube (synthetic lubricant)
- NyoGel 760G (vibration damping grease)
- Silicone grease
- 3M Marine Fast Cure Adhesive Sealant (for waterproofing)

Tail Segment

- 7 × M2 screws with matching nuts

4.2 Mechanical Structure

4.2.1 Head

The head is made up of three sections that are all printed using PLA. The front section houses the battery, the power switch, and assorted wires. This section also has future potential to incorporate a sonar sensor, a depth sensor, and a microphone for remote acoustic control. The mid-section of the head holds the ESP32 and voltage regulator mounted to a perf board within the water-tight compartment. A rubber O ring is placed within the lining of the cover and given a layer of silicone grease to ensure that the board is completely sealed away from any water. As for the back end of the head, it is a housing for a future depth control mechanism, which would be made from a syringe and a lead screw driven by a DC motor. All of these parts are held together using M2 screws and nuts in the protrusions seen on the outer edges. The screws holding the cover and control compartment together are lined with Threadlocker to prevent screws from getting loose and adds extra pressure on the O-ring.

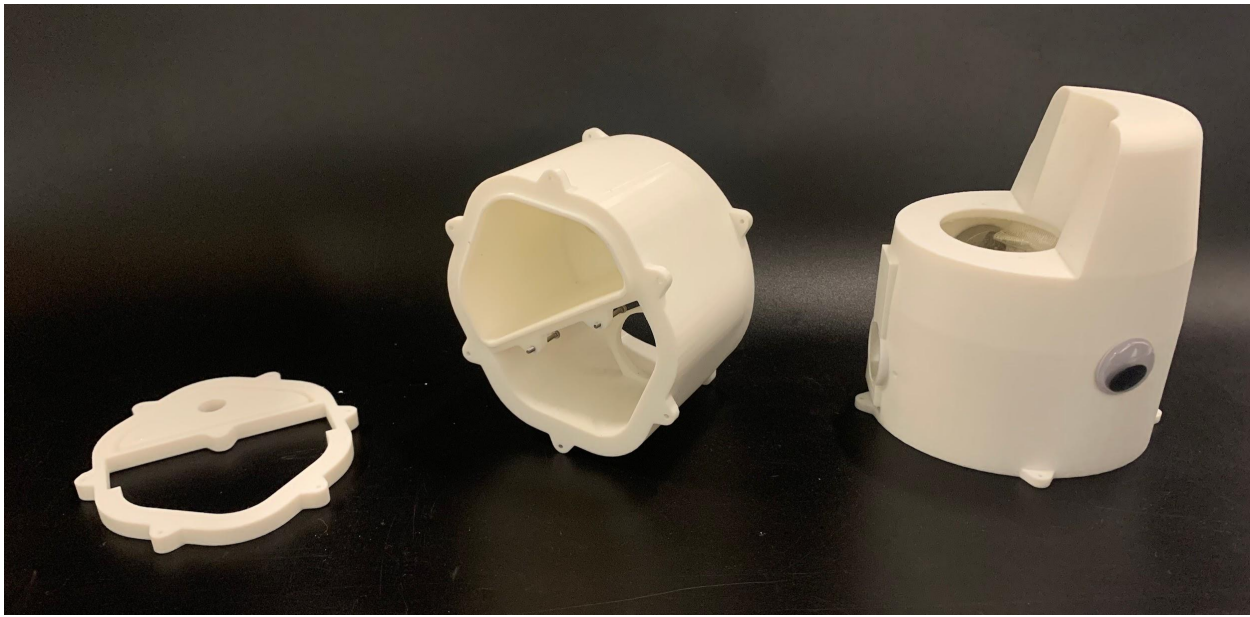


Figure 4.1: The cover, board compartment, and battery compartment of the head



Figure 4.2: The fully assembled head, including the housing for depth control

4.2.2 Modules

The three active modules are split into 3 sections: the active end, the flexible accordion midsection, and the passive end. The active end is mostly made out of 3D printed PLA parts, with the exception of the servo, screws, and heat set inserts. The servos are held in place by the spacer between the modules, which also acts as a place to attach foam and weights to adjust buoyancy. The actuation mechanism found within each module consists of the servo, a PLA spool, and a string. As the servo rotates in each direction, it turns the spool and pulls the string along with it. Each spool (shown in Figure 4.4) has two small pegs found 90° apart on the inner edge of the rim, which keep the strings in line while also acting as the main source of tension. To aid in keeping the strings tight, we decided on wrapping the strings around the spools 1.5 times, which would increase the overall friction. We chose to use string as our cable over something like a fishing line because it had some stretchability and was not terribly difficult to tie knots with. The accordion midsection of the modules is printed out of NinjaTech Chinchilla TPE, a very light and flexible material. The passive end of the module is printed out of PLA and acts as both the tying point for the strings and as a connection to the next module.

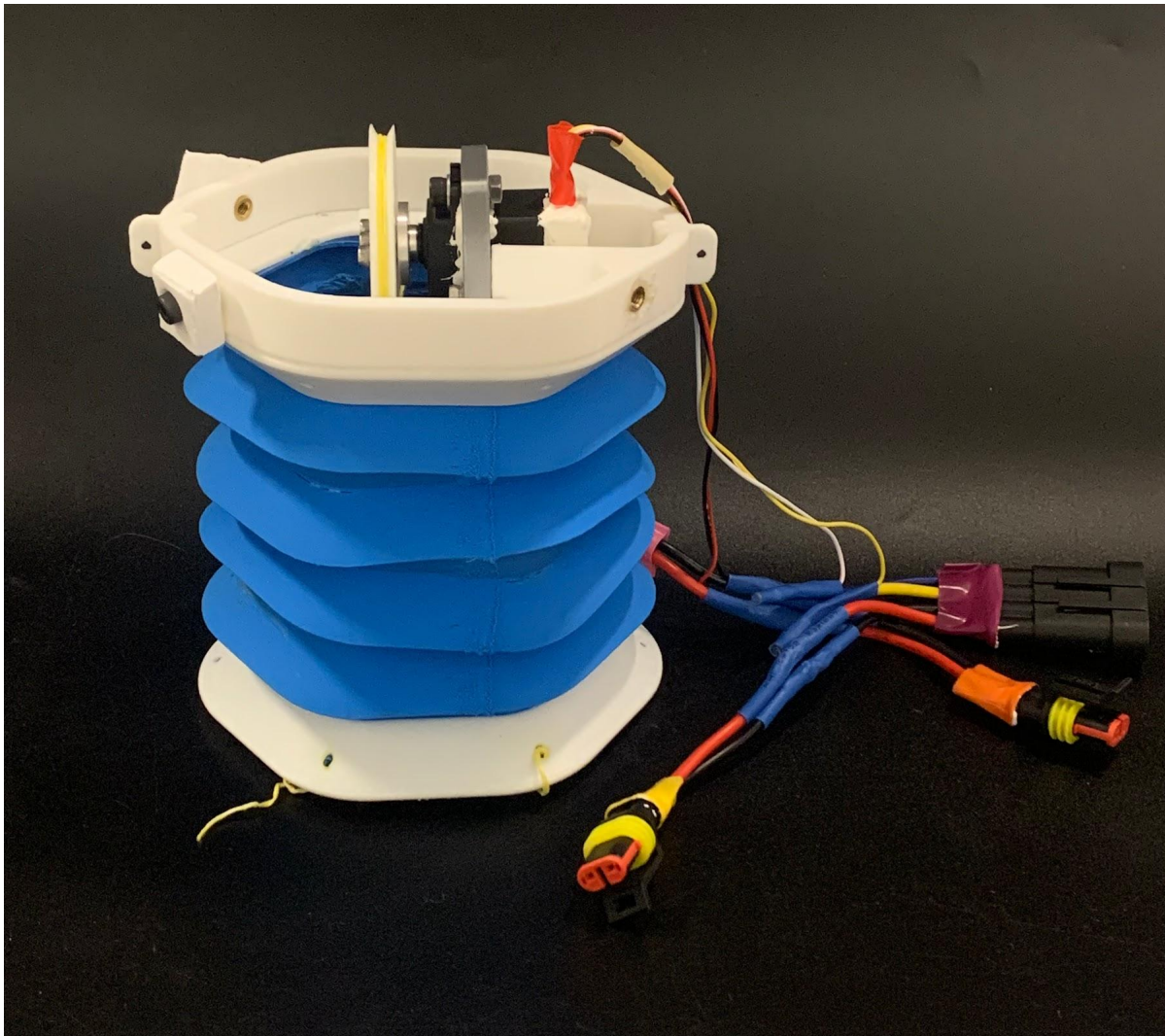


Figure 4.3: Complete body module

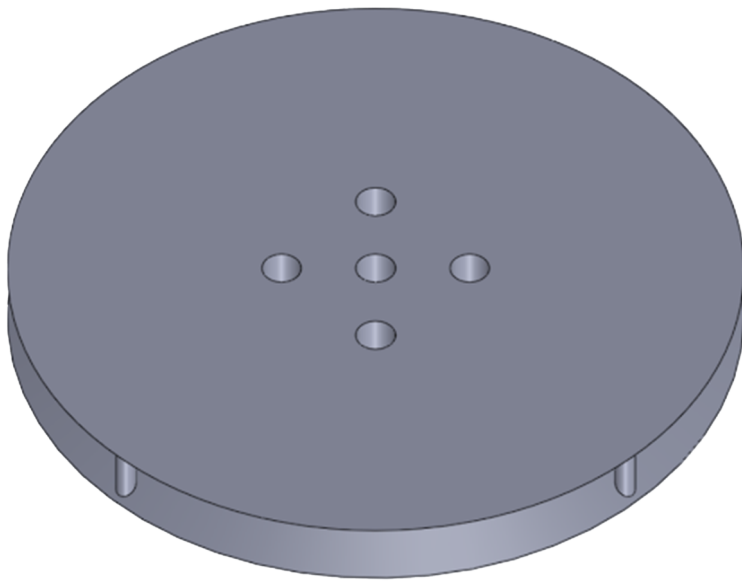


Figure 4.4: CAD model of the spool

4.2.3 Tail

As for the tail, it is printed out of a slightly more rigid TPE called NinjaFlex. It is intended to be fully passive and has holes in its mount to allow water to enter and exit the eel for buoyancy and draining.

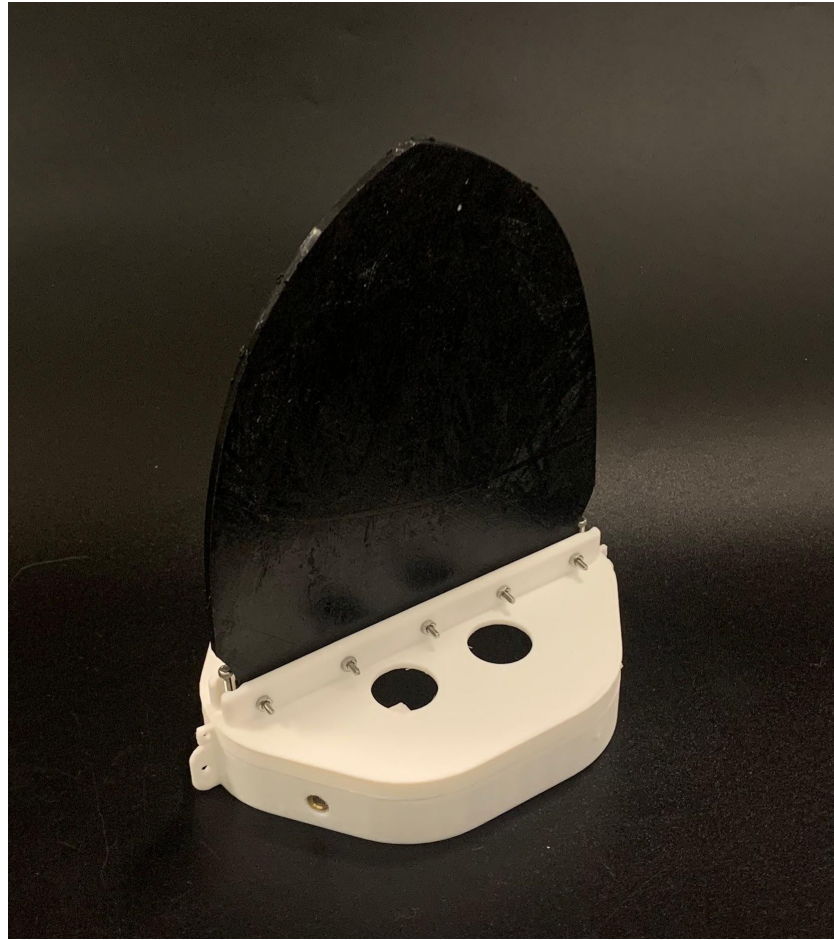


Figure 4.5: Passive Tail Assembly and Mount with Drainage and Buoyancy Holes

4.2.4 Fins

In order to add a level of stability and aid in propulsion, we designed a pair of fins to be attached to the top and bottom of our robot's modules. Each fin is made of NinjaTech Ninjaflex, and is segmented into two fitting pieces to allow for ease of printing. In order to combine the two parts, they needed to be soldered together. To attach them to the robot, mounting screw holes were added to the ends of each module, and holes were poked through the fins.

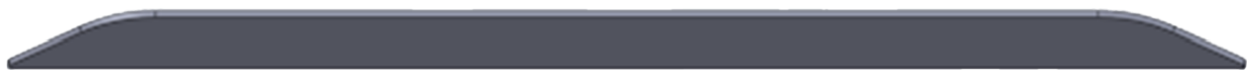


Figure 4.6: CAD model of one of the fins

4.3 Electronic Design

4.3.1 Control Board

The control board is a vital component of our eel, as it is what is responsible for controlling all of the servo motors as it swims. We selected our board based on two conditions: size and number of pins. Since we would be using 3 servo motors that required both a control and feedback wire to function, the board would need to have enough pins to support them all. The size was also a concern for us as we discovered quite early that there was a very limited amount of space inside the watertight compartment of the head, and we would have to be very picky to prevent the need to increase the overall length of the head. Taking all of this into consideration, we chose to use the ESP32. As an extra precaution for waterproofing, the perf board and ESP32 were coated with a layer of silicone grease that could be removed if changes needed to be made.

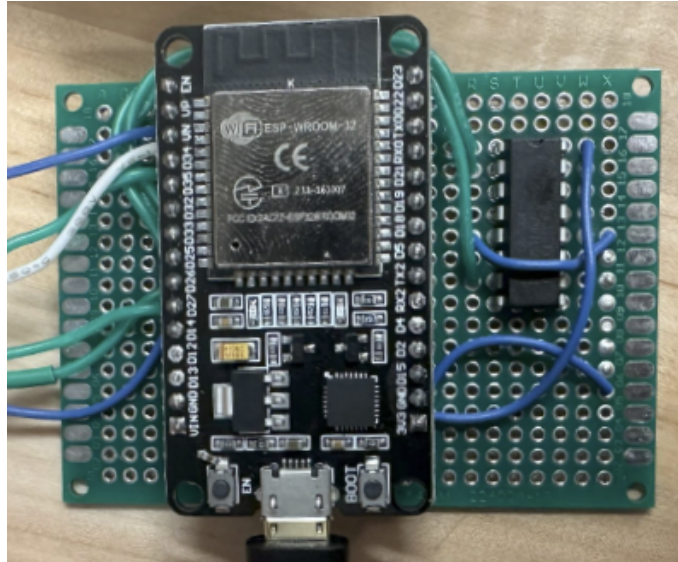


Figure 4.7: Perf board, ESP32, and L293D

4.3.2 Wiring

To support both modularity and waterproofing, we used waterproof cable connectors between each module, as shown in Figure 4.8. While these connectors were essential to meet our

functional goals, their bulky shape often led to mechanical interference. In particular, they occasionally pressed against the servo spools or became entangled with the tendon strings. Despite these drawbacks, the connectors were effective in enabling segment isolation and electrical continuity.

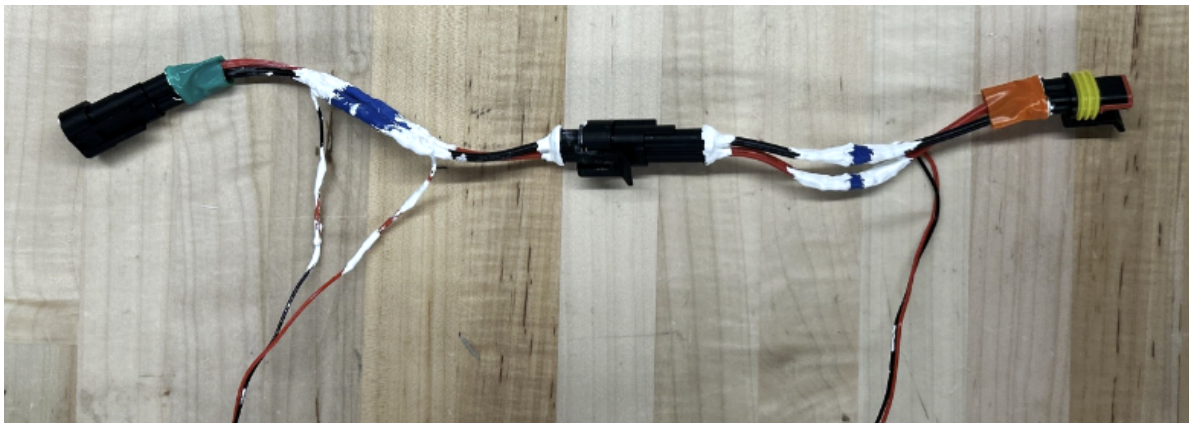


Figure 4.8: Wire connections found in each module

An overview of the full wiring harness prior to assembly is shown in Figure 4.9, illustrating how the connectors interface across modules. Additionally, Figure 4.10 presents the wiring diagram used as the basis for our circuit layout and signal routing.

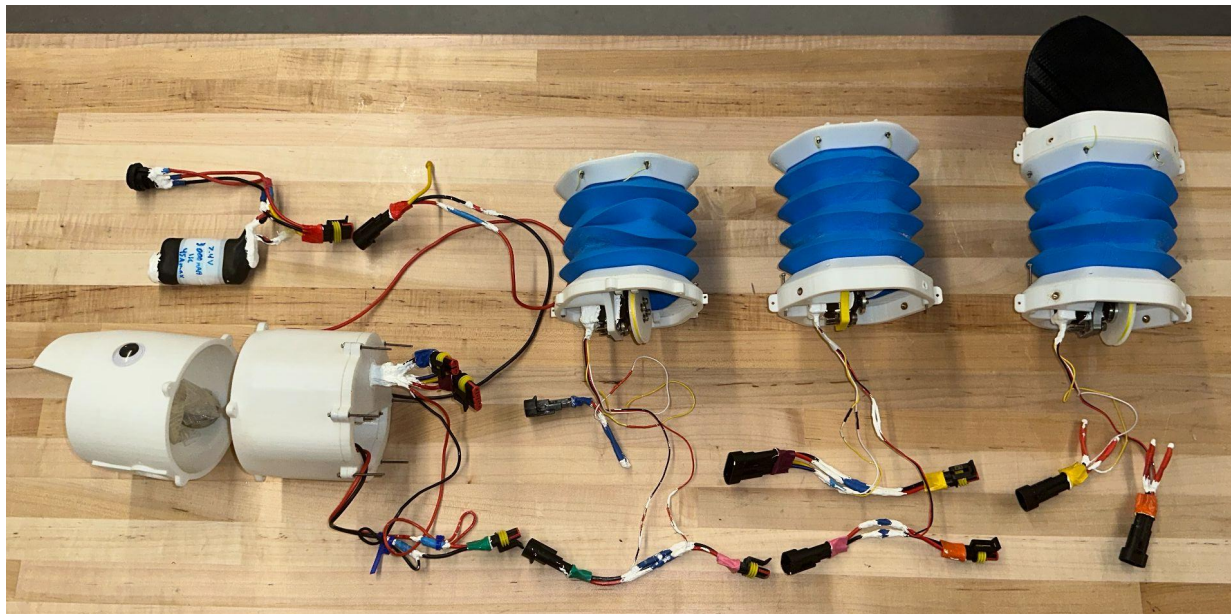


Figure 4.9: Full wiring layout including waterproof connectors and assembled segments

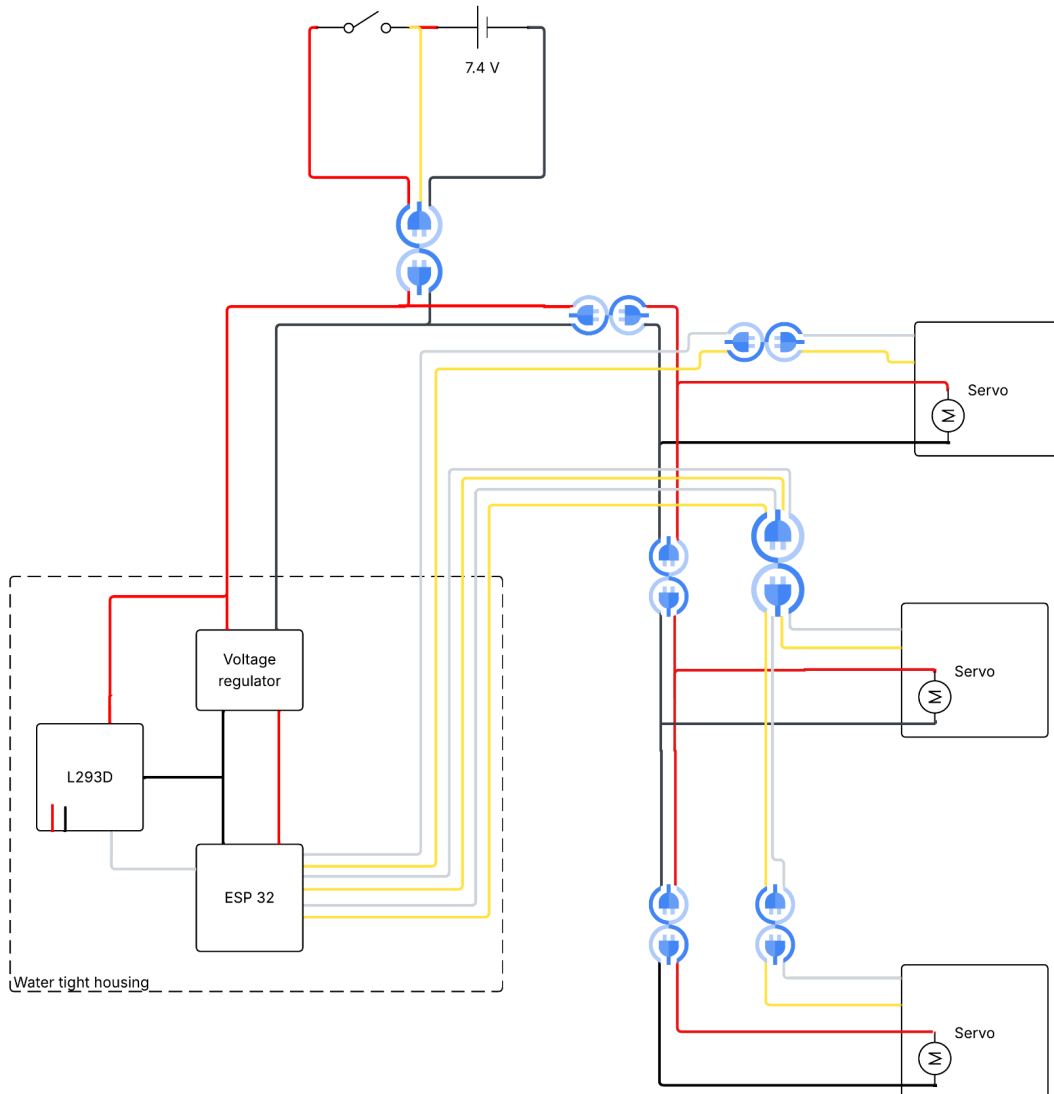


Figure 4.10: Wiring diagram used for signal and power distribution throughout the robot

4.3.3 Servo Motors

It was important to us that we maintain a level of accuracy when controlling the motion of the modules. We needed to have a motor that had a full range of motion, absolute encoders, and a high enough torque to be able to bend the modules easily. Our final choice was to use the Parallax Feedback 360° High Speed servo motors, as they were capable of fulfilling all of the requirements.

To keep each motor safe from water damage, we followed a very particular process that ensured the protection of individual components on the inside. Figure 4.11 depicts these steps in order, as well as which sealants were added to particular locations along the way. We started by removing the external screws and removing the top cover and the gears found just underneath them. Silicone grease was then applied to the screw holes. For the gear shafts, NyoGel was applied to the main shaft, while Super Lube was applied to the others. After placing the gears back in their proper place, the same sealants were then applied to their respective gears. The cover was then reapplied to the top of the motor, and the area around the protruding shaft was coated in silicone grease, fitted with an o-ring, and given another coating of silicone grease. Next, the underside of the motor was uncovered, exposing the electronics. From here, both the DC motor and electronics were desoldered and removed. A thinner layer of silicone grease was then added to the electronics to minimize the risk of overheating while still keeping it protected. The motor and electronics were then placed back in their initial positions and re-soldered. After closing up the bottom of the motor, silicone grease was applied to the screw holes and the screws were put back in their places. Lastly, all of the seams, screws, and the wire connector were covered in 3M Marine Fast Cure Adhesive Sealant.

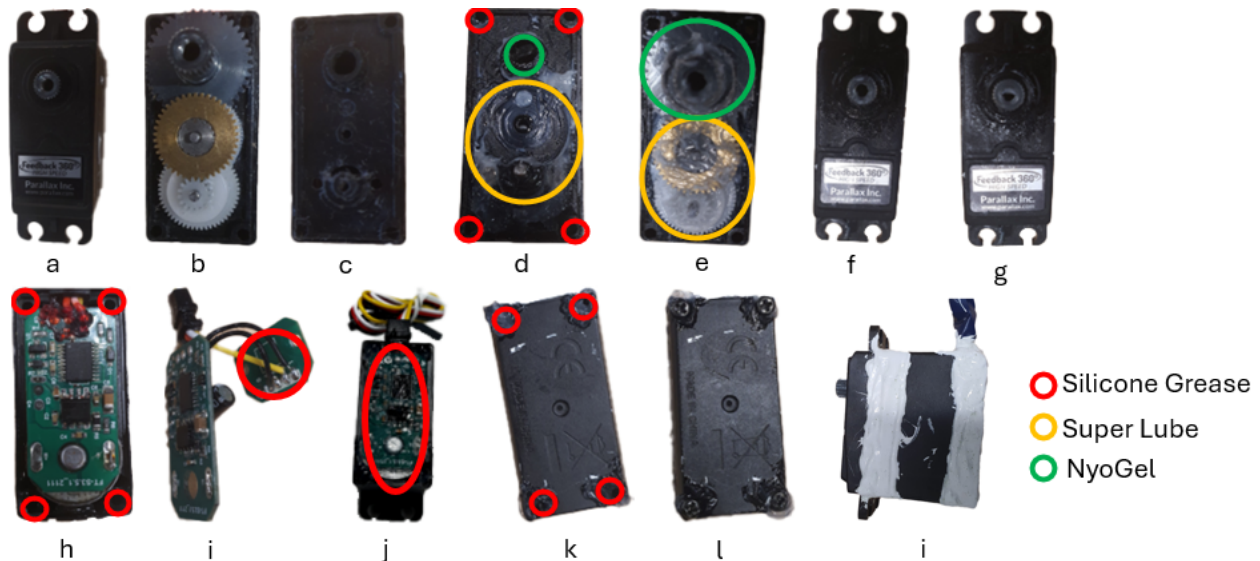


Figure 4.11: Steps to seal each motor, and the placement of each sealant

4.3.4 Battery

To keep the eel from being tethered while in use, we needed to incorporate a battery into the body. This battery needed to be capable of powering both the ESP32 as well as all three of the servo motors for a significant amount of time. After researching the voltage and current

requirements for each of the components, we chose to use a PCEONAMP Lithium-Ion battery with 7.4V, 3000mhA, and 45A. To ensure that this battery did not short out in the water, we waterproofed it by covering it in heat shrink and sealing off the ends of the tube with 3M Marine Fast Cure Adhesive Sealant as shown in Figure 4.12. As a means of making it easier to connect and disconnect batteries from the robot, we replaced the given wire connector with one of our waterproof ones, and incorporated a transistor switch so we could easily turn the robot on and off.



Figure 4.12: The fully waterproofed battery

4.4 Applications

While in the designing process, we tried to come up with ways in which to allow future groups to easily modify and expand upon what we had created. This is how we decided to make the robot modular, as well as making space to implement sensors. Making the robot modular makes it possible to add or subtract sections, as well as making it much easier to replace damaged motors. In addition to designing for future expansion, we also kept in mind where the robot could be used. By incorporating places for sensors and a depth control device, later iterations of the eel could find use as a means of exploring shipwrecks and undersea wildlife, while causing less of a disturbance than traditional robotics.

5 TESTING AND RESULTS

5.1 Accordion Material Testing

To improve the module bend angle, our team tested 2 different flexible materials: Ninjaflex TPE and NinjaTek Chinchilla. To test both materials, a special mount was 3D printed that allowed us to keep a single body module positioned upright, not vertically standing on end, but oriented how the eel swims, so that we could view a more natural bend with more accurate gravitational pull. Markers were placed on the hex caps which were then placed onto the accordions and attached to the mount. The body module was filmed as it bent in both directions. The video was then uploaded into Physlet Tracker and used to determine the x and y coordinates of the trackers at the maximum bend angle in both directions. Finally, the x and y coordinates were used to calculate the bend angle, along with other bending properties, based on the geometry in Figure 5.2, using the following equations:

$$\text{Curvature: } \alpha = \cos^{-1}\left(\frac{x}{\sqrt{x^2+y^2}}\right)$$

$$\text{Bend Angle: } \theta = 2\left(\frac{\pi}{2} - \alpha\right)\left(\frac{180^\circ}{\pi}\right)$$

$$\text{Radius: } r = \frac{x^2+y^2}{2x}$$

$$\text{Arc Length: } l = \theta r$$

It is important to note that these bend angles are not the same bend angle as the one calculated in SolidWorks during the accordion design process, which was based on the angle formed by the faces of the hex caps

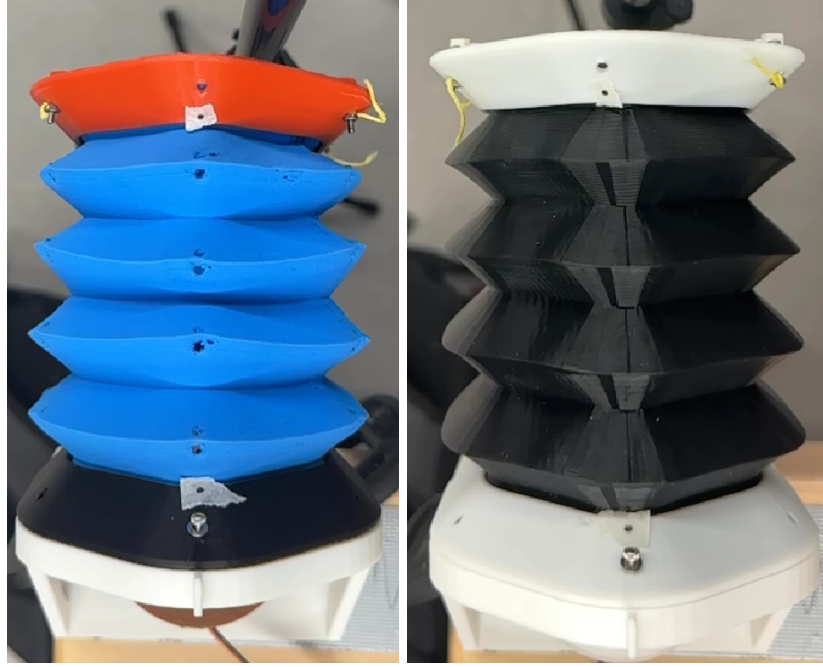


Figure 5.1: Body modules made of Chinchilla (left) and Ninjaflex (right) set up for bend angle testing

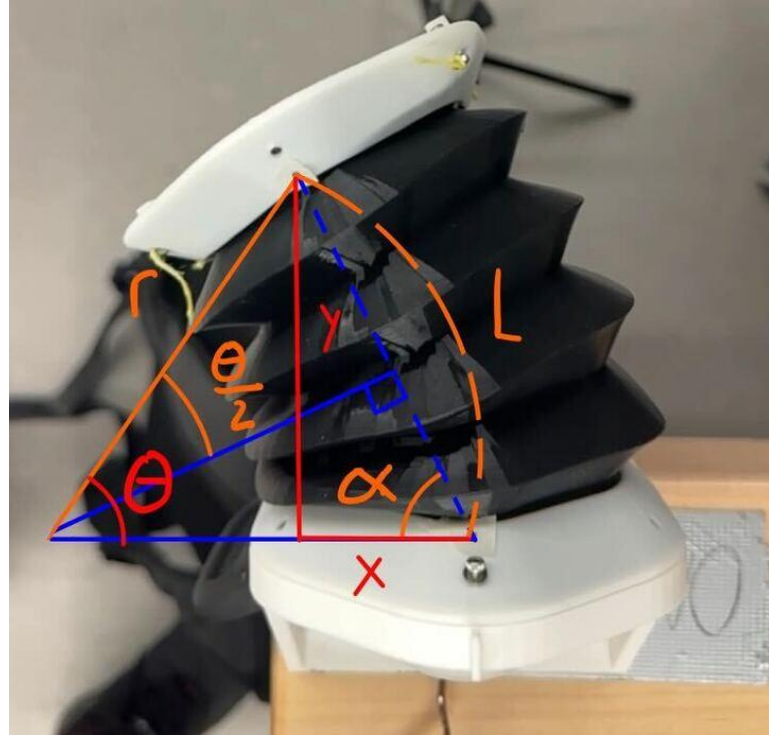


Figure 5.2: Diagram of the geometry utilized to calculate bend angle (θ)

Material	Direction	Bend Angle (deg)	X position (mm)	Y position (mm)	Radius (mm)	Arc Length (mm)
NinjaFlex	Left	44.5	34.55	84.27	120.29	93.51
NinjaFlex	Right	41.8	34.12	89.43	134.26	97.87
Chinchilla	Left	69.0	32.81	47.77	51.18	61.60
Chinchilla	Right	72.3	32.49	44.45	46.65	58.89

Table 5.1: Table of results from testing body module bend angles with accordions made from Chinchilla and NinjaFlex

From these tests, it was clear that the Chinchilla filament provided a greater bend angle, which is why we chose to use it as the material for our accordions.

5.2 Spool String Wraps

Our research showed that increasing the number of wraps of a string around the spool exponentially increases the friction between the string and the spool, decreasing the slippage. However, the number of wraps also increases the load on the motor. Hence, tests were needed to find the optimal way to wrap the spool to maximize the bend angle of the modules. The string was wrapped around the spool 0.5, 1.5, and 2.5 times. Then the body model was set up using the same process as in the accordion materials testing (See above)

Testing and Results

Spool Wraps	Material	Direction	Bend Angle (deg)	X position (mm)	Y position (mm)	Radius (mm)	Arc Length (mm)
0.5	Chinchilla	Left	40.4	22.06	59.97	92.54	65.24
0.5	Chinchilla	Right	38.7	21.18	60.35	96.57	65.19
1.5	Chinchilla	Left	55.3	26.08	57.38	76.16	64.98
1.5	Chinchilla	Right	47.2	23.98	61.89	91.86	67.91
2.5	Chinchilla	Left	48.9	27.82	53.1	64.59	62.34
2.5	Chinchilla	Right	42.4	24.27	55.52	75.64	62.34

Table 5.2: Table of results from testing body module bend angles with different amounts of spool wrapping

5.3 Servo Amplitude/Speed Testing

To evaluate the impact of servo amplitude on swimming performance, we programmed the robot to swim at amplitudes ranging from 90° to 115° , in 5° increments. The frequency of oscillation was held constant at 1.25 Hz to match both the previous eel design and the typical swimming frequency of biological eels. For each test, the servo control function was adjusted to the target amplitude, and the eel was allowed to swim for 30 seconds. Between trials, the robot was returned to its neutral (centered) position to ensure consistent starting conditions. This testing was filmed in an Olympic swimming pool (as shown in Figure 5.3), with a GoPro camera placed on the bottom of the pool at a depth of 4 feet. These videos were then uploaded to and analyzed in Physlet Tracker to determine the speed at which the eel moved during these tests.

Testing and Results

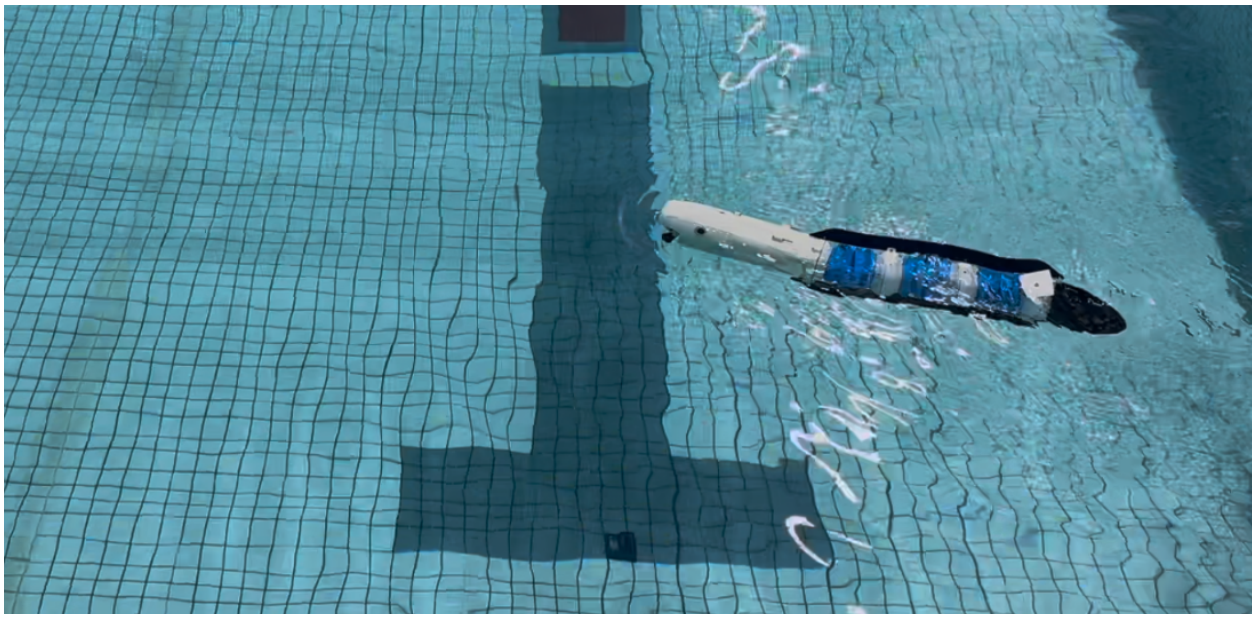


Figure 5.3: Pool testing of the soft robotic eel during servo amplitude trials

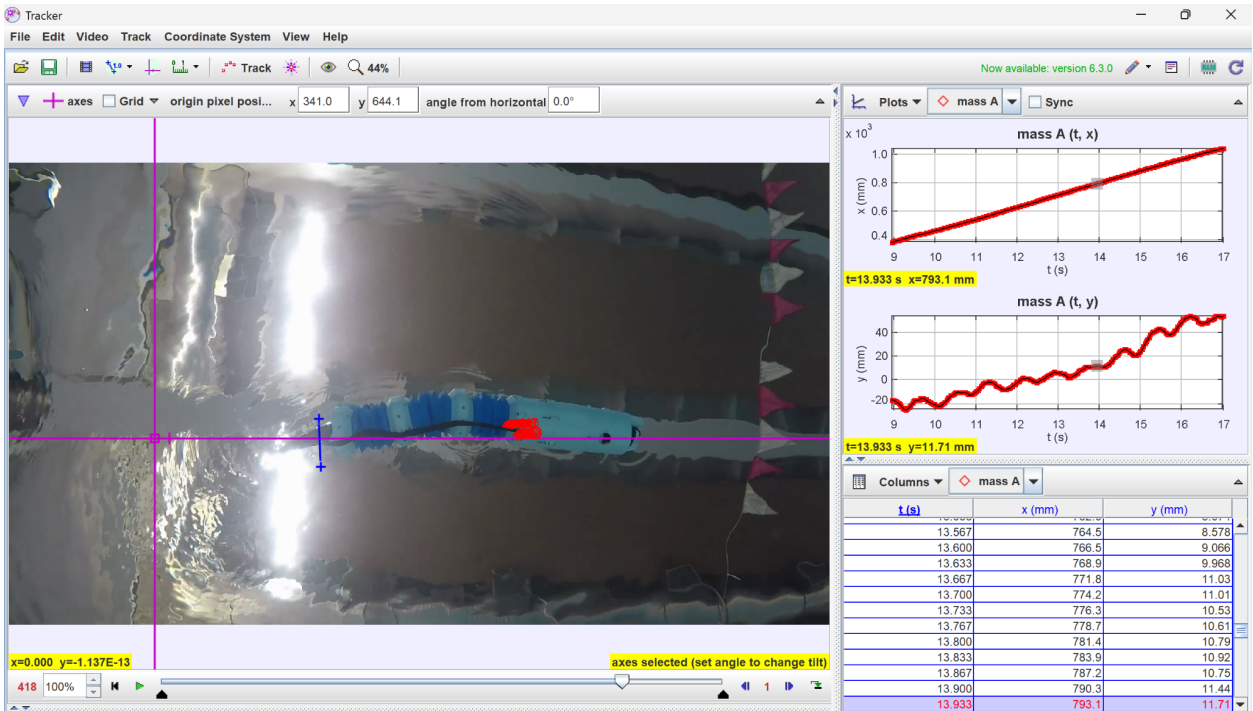


Figure 5.4: Screenshot of Physlet Tracker being used to determine Eel speed

Testing and Results

Amplitude	Start X	Start Y	End X	End Y	Start Time	End Time	Distance (mm)	Speed (mm/s)	Speed (BL/s)	Speed (mm/s)
90	381.4	-425.4	1024	-126.7	11.5	17.667	708.629981	114.9	0.141	114.9
95	352.1	352.1	891.6	61.74	7.2	12.5	612.67	115.6	0.142	115.6
100	394.9	-481	1134	-85.65	6.467	13.533	838.19	118.6	0.146	118.6
105	220.5	-393.2	940.7	103.9	4.267	11.467	875.10	121.5	0.149	121.5
110	569.4	-241.7	798.7	-91.89	7.2	9.267	273.90	132.5	0.163	132.5
115	-253.4	-540	95.05	-669.3	1.6	4.333	371.67	136.0	0.167	136.0

Table 5.3: Table of data collected from Servo Amplitude vs Speed Testing

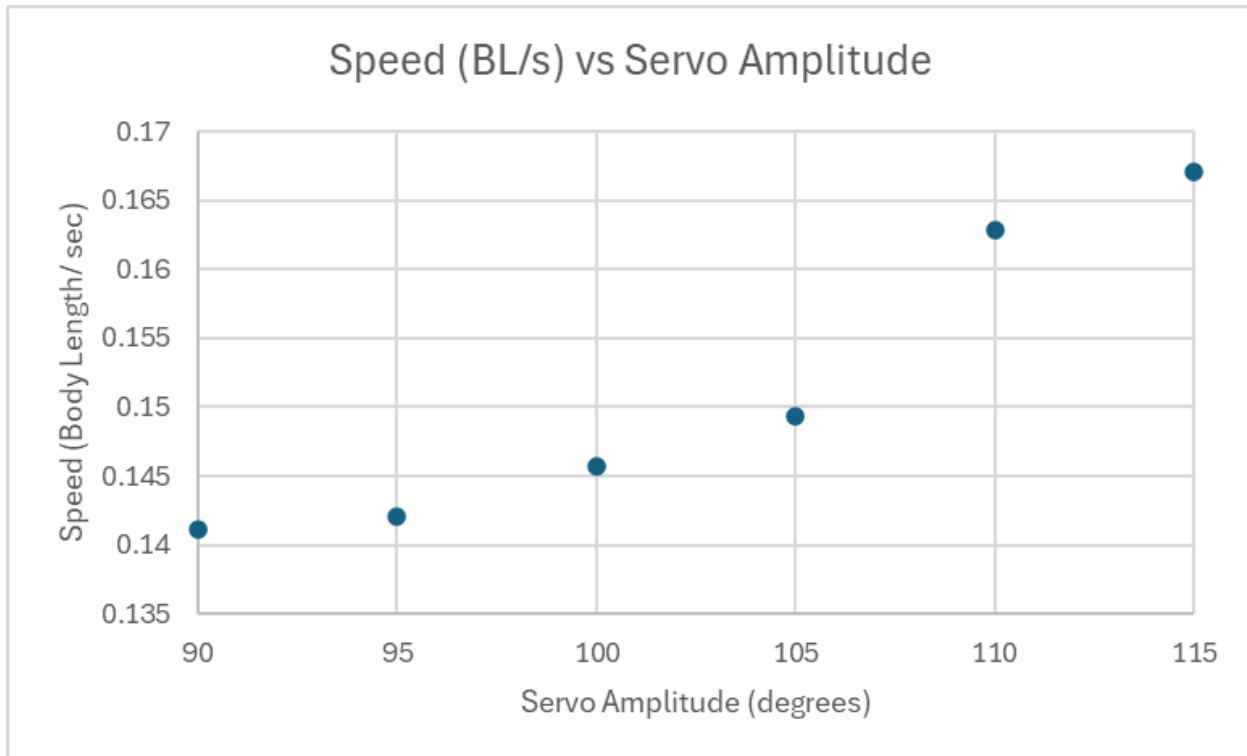


Figure 5.5: Graph of eel speed in body lengths per second vs the servo amplitude in degrees

This test revealed a clear positive correlation between servo amplitude and swimming speed, consistent with the findings of Dr. Hall's earlier work [16]. However, the results were inconclusive in determining the robot's maximum speed. While increasing amplitude generally led to faster swimming, we expect this trend would eventually plateau or even reverse. At a certain point, the physical limitations of the system would prevent further increases in bend angle, even if the commanded servo amplitude continues to increase. At this point, the system would reach its top speed. Since this threshold was not encountered during these tests, the eel's maximum speed remains unknown.

6 DISCUSSION

6.1 Comparison to Previous Eel

When tasked with developing the eel, we were told to take inspiration from and improve upon the past work of one of our advisors. To prove that we have accomplished this task, we will be comparing qualitatively as well as quantitatively the results of our work. In terms of modularity and scalability, our design far exceeds that of the original, as there was no room in the original for additional functionality or an easy way to modify it. Despite our initial concerns with the lack of durability that our accordions offered, once we were able to fortify the material it proved to be more durable overall than the original. Not to mention that our parts are much easier to replace within the structure, assuming they can be reproduced properly. Looking into the performance of our design, at its peak, it traveled at about 84% the speed of the original with respect to body lengths per second. However, after looking into the data for our results, it should be noted that our speed did show continuous growth. This means that our design has the potential to surpass the original, provided further improvements are made.

6.2 Challenges

One of the main challenges we faced was with printing the accordions. There was only one 3D printer capable of working with the TPE filament we had chosen to use. While it did manage to get the job done, it took a lot more effort to fabricate the accordions. Each print needed to be watched very carefully, as they had a very high tendency of failing at just about any point. Because of this, once we had created sufficient versions to use in testing the modules as a whole, we opted to stop trying to replace them and instead found various ways in which to make quick repairs when needed.

7 RECOMMENDATIONS

7.1 Overview

While this project proved a valuable educational experience to all those involved, it does not in and of itself provide a significant advancement in the field of soft aquatic robotics. Instead, the scholarly relevance of this robot lies in its future uses as a platform for more advanced robotics and potential future use in aquatic exploration and research. There are a number of improvements that could be made to make the eel a more reliable platform for these future innovations in soft robotic design and applications.

7.2 Mechanical Design

The primary mechanical limitation was the fragility of the accordion segments. While the Chinchilla filament enabled soft, flexible motion, it lacked the durability needed for repeated handling and underwater operation. Tears often occurred around mounting points, and repairs involved melting the material back together with a soldering iron. This was a workaround that functioned temporarily but was not a long-term solution. In the future it would be smart to explore alternative materials such as silicone or silicone-coated flexible prints to increase resilience without sacrificing flexibility. A more robust material might also open up options for increased internal space and stronger motors, assuming we could balance those upgrades with budget and waterproofing constraints.

When we switched to feedback servos mid-project, the mechanical design had to be adapted, resulting in the spool being slightly off-center within the accordion. A potential consideration would be a revision of the segment geometry, and potentially scaling the entire system, which could better center the spool and improve actuation symmetry. However, the string and servo mounting system performed reliably and would likely scale well with improved segment design.

In addition, our lack of strict planning early on led us to neglect designing a proper housing for any kind of battery. In the future, it should be noted that the best place to house a

battery is somewhere inside the head, as holding the weight there will have the smallest impact on the movement overall.

7.3 Electronic Hardware

Despite these successes, several limitations impacted our electronic setup's performance and maintenance. The perf board and connectors were particularly fragile and presented significant challenges in waterproofing due to their exposed nature and limited internal space within the eel's head. Future developments should prioritize transitioning from a perf board to a custom-designed printed circuit board (PCB). This change would significantly streamline wiring, improve reliability, and simplify waterproofing efforts.

In addition, internal wiring was complex, often routed behind motors, causing difficulty in maintaining a clean, organized internal structure. These constraints limited modularity and ease of maintenance. Adopting more compact and robust waterproof connectors would enhance the modularity and ease of maintenance. Improved internal wire routing and the implementation of strain relief would also facilitate better structural organization, allowing additional space for sensor integration and more robust electronics.

Wiring could also be simplified and allow for complete interchangeability of modules and expandability by utilizing I2C communication to control and get feedback from the motors. This would allow the wiring to be identical between modules.

7.4 Controls

While effective for basic motion tests, this open-loop approach limited the system's flexibility and adaptability. The absence of real-time gait adjustments, reactive behaviors, and steering significantly restricted the robot's capabilities. Without sensor input or feedback from the servos, the eel could not correct its path or respond to environmental conditions dynamically. Enhancing the control system in future iterations should involve transitioning to a closed-loop design. Currently, the front compartment has places in which to house a depth sensor, microphone, and ultrasonic sensor. This should serve as a relatively baseline starting point for sensor implementation.

Our team attempted to implement a buoyancy control device utilizing a lead screw actuated syringe, but had to abandon the device due to time constraints. The L293D motor driver is also already mounted and wired on the perf board and can be used to drive this actuator.

Implementation of this device would significantly increase the practicality of this platform. Specifically redesign the device with proper sealing and get the electronics actually functioning.

Integrating sensors such as sonar for obstacle detection, depth sensors for vertical position control, and a microphone for acoustic communication would vastly increase the robot's autonomy and functional versatility.

Implementing a real-time feedback mechanism using servo positional data would enable dynamic gait tuning and steering adjustments, allowing the eel to respond effectively to changing environmental conditions and user commands.

Another major upgrade would be integrating SURF-COM, an acoustic communication interface developed by one of our team members and our advisors in the Soft Robotics Lab, as this would allow wireless control and parameter adjustment via acoustic signals. By incorporating a microphone into the electronics system, future iterations of the eel could receive commands or updated parameters underwater, without relying on physical tethering or pre-programmed behaviors. This would significantly enhance the system's responsiveness and potential for remote or semi-autonomous operation in submerged environments.

7.5 Future Exploration

Once the eel reaches a level of development that a future team deems capable of exploring new domains, we propose several potential directions for the project's continued evolution. With the integration of more advanced sensors, one promising avenue would be to adapt the eel for underwater terrain mapping and surveying. The incorporation of cameras and ultrasonic sensors would enable the collection of high-resolution imagery and accurate topographical data, respectively.

Alternatively, by enhancing the eel's realism—both in appearance and in biomimetic movement—it could serve as a discreet observational tool for aquatic life. This would allow researchers to study species, such as eels, in their natural habitats without disrupting typical behaviors. Such a system could be particularly valuable for monitoring breeding habits and life cycles.

Additionally, the eel could be repurposed to assess the health of sensitive ecosystems, such as coral reefs. Deploying a robotic system in these environments would minimize human interference while enabling continuous, detailed observation.

8 CONCLUSION

The development of our soft robotic eel was driven by three primary objectives: enhance modularity, increase mechanical performance, and enable future expandability. To meet our goal of modularity, the implementation of wire connectors and a system of individual segments achieved a level of modularity that represented a significant improvement over the original design. While the system offered improved modularity, it remained time-consuming to access certain key components, such as the ESP32, which required frequent access during code uploads and debugging. Overall, it was vastly more modular than the original design. As for increasing mechanical performance, direct comparison to previous iterations was limited, since we could not properly compare the two versions. However, the eel's observed speed indicates encouraging progress, as our data showed promising signs of further potential. When it comes to our goal of future expandability, the current system lays a strong foundation for continued development. The head segment offers opportunities for integration of additional sensors and depth control capabilities; modules themselves could benefit from more durable materials, and further means of modularity are possible through the use of more advanced connectors and the incorporation of an I2C communication protocol, as appropriate. Overall, we achieved a significantly higher degree of modularity, demonstrated promising mechanical performance, and established a strong foundation for future expandability in soft robotic systems.

8.1 Importance

While many underwater robots today are designed as rigid-bodied systems with straightforward functionality, it is clear that soft robotics often goes overlooked. Flexible, natural movement can offer key advantages in environments where traditional designs fall short. A fully developed version of our robot could access environments that rigid systems cannot, making its potential applications particularly compelling. Our hope is that this project fosters an interest in others for the fascinating aspects in such a field of robotics. Whether the goal is to avoid disturbing marine life, explore sunken structures, or explore concepts inspired by biomimetic design, soft robotics has much to offer in aquatic environments.

REFERENCES

- [1] B. L. Southall, A. E. Bowles, W. T. Ellison, J. J. Finneran, R. L. Gentry, C. R. Greene Jr., D. Kastak, D. R. Ketten, J. H. Miller, P. E. Nachtigall, W. J. Richardson, J. A. Thomas, and P. L. Tyack, “Overview,” *Aquatic Mammals*, vol. 33, no. 4, pp. 411–414, 2007, doi: 10.1578/AM.33.4.2007.411.
- [2] R. K. Katzschmann, J. DelPreto, R. MacCurdy, and D. Rus, “Exploration of underwater life with an acoustically controlled soft robotic fish,” *Science Robotics*, vol. 3, no. 16, p. eaar3449, 2018, doi: 10.1126/scirobotics.aar3449.
- [3] C. Laschi, B. Mazzolai, and M. Cianchetti, “Soft robotics: Technologies and systems pushing the boundaries of robot abilities,” *Science Robotics*, vol. 1, no. 1, p. eaah3690, 2016, doi: 10.1126/scirobotics.aah3690.
- [4] A. Jusufi, D. M. Vogt, R. J. Wood, and G. V. Lauder, “Undulatory swimming performance and body stiffness modulation in a soft robotic fish-inspired physical model,” *Soft Robotics*, vol. 4, no. 3, pp. 202–210, 2017, doi: 10.1089/soro.2016.0053.
- [5] A. D. Marchese, R. K. Katzschmann, and D. Rus, “A recipe for soft fluidic elastomer robots,” *Soft Robotics*, vol. 2, no. 1, pp. 7–25, 2015, doi: 10.1089/soro.2015.0002.
- [6] Z. Chen, W. Jiao, K. Ren, J. Yu, Y. Tian, K. Chen, and X. Zhang, “A survey of research status on the environmental adaptation technologies for marine robots,” *Ocean Engineering*, vol. 286, p. 115650, 2023, doi: 10.1016/j.oceaneng.2023.115650.
- [7] F. Plum, S. Labisch, and J.-H. Dirks, “SAUV—A bio-inspired soft-robotic autonomous underwater vehicle,” *Frontiers in Neurorobotics*, vol. 14, p. 8, 2020, doi: 10.3389/fnbot.2020.00008.
- [8] J. Stin, “Form and function of anguilliform swimming,” *Biological Reviews*, vol. 99, no. 2, pp. 345–367, 2024, doi: 10.1111/brv.13116.
- [9] A. J. Smits, “Undulatory and oscillatory swimming,” *Journal of Fluid Mechanics*, vol. 874, p. P1, 2019, doi: 10.1017/jfm.2019.284.

References

- [10] E. D. Tytell and G. V. Lauder, “The hydrodynamics of eel swimming,” *Journal of Experimental Biology*, vol. 207, no. 11, pp. 1825–1841, 2004, doi: 10.1242/jeb.00968.
- [11] G. B. Gillis, “Environmental effects on undulatory locomotion in the American eel (*Anguilla rostrata*): Kinematics in water and on land,” *Journal of Experimental Biology*, vol. 226, no. 5, p. jeb245678, 2023, doi: 10.1242/jeb.245678.
- [12] O. Perera, R. Liyanapathirana, G. Gargiulo, and U. Gunawardana, “A review of soft robotic actuators and their applications in bioengineering, with an emphasis on HASEL actuators’ future potential,” *Actuators*, vol. 13, no. 12, p. 524, 2024, doi: 10.3390/act13120524.
- [13] Y. Li, Y. Xu, Z. Wu, and Y. Li, “A comprehensive review on fish-inspired robots,” *International Journal of Advanced Robotic Systems*, vol. 19, no. 3, pp. 1–20, 2022, doi: 10.1177/17298814221109744.
- [14] T. Wang and K. H. Low, “Modeling and analysis of undulatory swimming for a biomimetic robotic fish,” *International Journal of Advanced Robotic Systems*, vol. 9, no. 4, p. 53, 2012, doi: 10.5772/51050.
- [15] J. Xu, X. Irigoien, and M.-S. Alouini, “State-of-the-art underwater vehicles and technologies enabling smart ocean: Survey and classifications,” *arXiv preprint arXiv:2412.18667*, 2024. [Online]. Available: <https://arxiv.org/abs/2412.18667>
- [16] R. Hall, G. Espinosa, S.-S. Chiang, and C. D. Onal, “Design and testing of a multi-module, tetherless, soft robotic eel,” in *Proc. 2024 IEEE Int. Conf. on Robotics and Automation (ICRA)*, Yokohama, Japan, 2024, pp. 8821–8827, doi: 10.1109/ICRA57147.2024.10611531.
- [17] Long Island Aquarium, “Moray Eel,” *Long Island Aquarium*. [Online]. Available: <https://www.longislandaquarium.com/exhibits/moray-eels/> [Accessed: May 1, 2025].
- [18] ScienceDirect Topics, “Anguilla (Eels) – an overview,” *ScienceDirect*. [Online]. Available: <https://www.sciencedirect.com/topics/agricultural-and-biological-sciences/anguilla-eels> [Accessed: May 1, 2025].
- [19] G. V. Lauder and E. D. Tytell, “Hydrodynamics of undulatory propulsion,” in *Fish Biomechanics*, J. E. Mittal, Ed. Amsterdam, Netherlands: Academic Press, 2005, pp. 425–468.
- [20] Florida Museum, “Green Moray – Discover Fishes,” *University of Florida*, 2025.

References

- [Online]. Available: <https://www.floridamuseum.ufl.edu/discover-fish/species-profiles/green-moray/> [Accessed: May 1, 2025].
- [21] D. Righton, H. Westerberg, E. Feunteun, F. Økland, P. Gargan, E. Amilhat, *et al.*, “Empirical observations of the spawning migration of European eels: The long and dangerous road to the Sargasso Sea,” *Science Advances*, vol. 2, no. 10, p. e1501694, 2016, doi: 10.1126/sciadv.1501694.
- [22] V. van Ginneken and G. Maes, “The European eel (*Anguilla anguilla*), its lifecycle, evolution and reproduction: A literature review,” *Reviews in Fish Biology and Fisheries*, vol. 15, no. 4, pp. 367–398, 2005, doi: 10.1007/s11160-006-0005-8.
- [23] F. W. Tesch, *The Eel*, 5th ed. Oxford, UK: Blackwell Science, 2003.
- [24] R. Zhang, W. Zhou, M. Li, and M. Li, “Design of a double-joint robotic fish using a composite linkage,” *arXiv preprint arXiv:2408.06666*, 2024. [Online]. Available: <https://arxiv.org/abs/2408.06666>
- [25] J. Yuh, “Design and control of autonomous underwater robots: A survey,” *Autonomous Robots*, vol. 8, no. 1, pp. 7–24, 2000, doi: 10.1023/A:1008948910448.